Interference Assisted Laser Induced Forward Transfer for Line Patterning

Ankur Shah

A Thesis

In

The Department

of

Mechanical and Industrial Engineering

Presented in Partial Fulfillment of the Requirements

for the Degree of Master of Applied Science (Mechanical Engineering) at

Concordia University

Montreal, Quebec, Canada

September, 2008

Library and
Archives Canada

Published Heritage
Branch

395 Wellington Street
Ottawa ON K1A 0N4
Canada

Bibliothèque et
Archives Canada

Direction du
Patrimoine de l'édition

395, rue Wellington
Ottawa ON K1A 0N4
Canada

Canada

ABSTRACT

Interference Assisted Laser Induced Forward Transfer for Line Patterning

Ankur Shah

Biomedical and microelectronic devices such as microinjectors and interconnects require line patterns to be fabricated on their surface. The process to pattern such surfaces should consider the requirements such as chemical inertness and biocompatibility. Laser Induced Forward Transfer (LIFT) is a simple direct write technique which offers the ability to pattern a substrate by localized deposition of material. In LIFT, a laser beam is focused through donor substrate (DS) coated with thin film to deposit on the acceptor substrate (AS) to be patterned. In this research project, a new laser based micropatterning method combining LIFT and laser interferometry for depositing periodic line patterns on a substrate has been proposed. Considering biocompatibility, glass has been selected as the acceptor substrate where a laser beam was focused on a gold film to get deposited on it.

Theoretical modeling has been done to predict the laser and optical parameters on the dimensions of the gold line patterns. Also the effect of refractive index and thickness of the DS on the patterned dimensions has been analyzed. Experiments were done to deposit patterns of widths ranging from 4 to 10 μm with the pitch between 8 and 20 μm. Experiments were also done by varying the feed rate and dwell time of scanning to achieve continuity in deposition and up to 700 μm in length i.e. three times the focused spot size have been deposited. With the proposed method, pattern dimensions on the substrate can be easily modified by making simple changes to the optical setup.

ACKNOWLEDGEMENTS

TABLE OF CONTENTS

LIST OF FIGURES

LIST OF TABLES

CHAPTER 1   INTRODUCTION

Surface patterning generally refers to the physical modification of the functional properties of the substrate surface by surface engineering. The reason for changing its structure and corresponding properties may be different and varied. The requirement could be to change the friction between the mating surfaces, or it could be improving biocompatibility or to change the wetting ability characteristics of a surface or to change the sensitivity of a surface to a given environment. Surface patterning plays an important role today and there are many pattern transfer techniques available, few of which have been discussed in next section.

1.1   Lithography

Patterning structures in field of microfabrication can be conventionally done by lithography. Lithography is a process in which pattern is transferred to a photosensitive material. The substrate to be patterned is covered with a layer of photoresist that is radiation sensitive, which when exposed to photosensitive material, changes its solubility properties. After exposure, the resist is developed in a suitable solution, and the desired pattern is created onto the substrate [1]. Fig 1.1 shows the process of conventional lithography. Photolithography i. e., the lithography using a light source (UV source), is by far the most widely used lithography technique in microfabrication [2]. Other methods used are electron beam, ion beam and X-ray lithography that have attracted considerable attention recently.

CONVENTIONAL
LITHOGRAPHY

1 LAYERING OF MATERIALS

Photoresist

Silicon dioxide

Silicon substrate

2 EXPOSURE TO
ULTRAVIOLET LIGHT

Mask

3 RESIST DEVELOPMENT
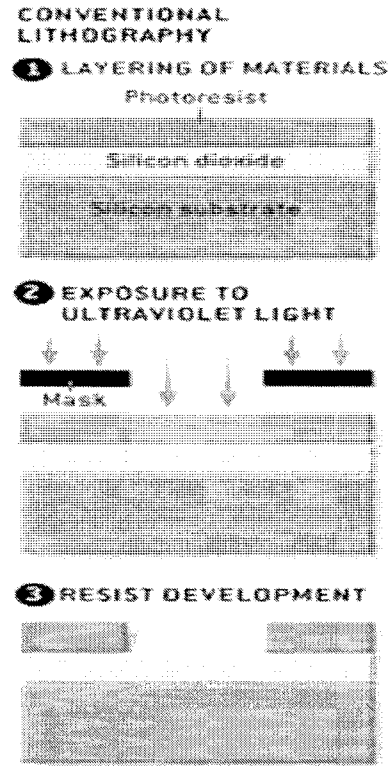
Fig 1.1 Schematic illustration of Conventional lithography [3]

1.1.1 Photolithography

In photolithography, the substrate is covered with a photoresist and a photomask is kept above it. With a positive photoresist, the bright parts of the mask, where the radiation gets through, cause the resist material to become soluble in a developer solution, while the dark parts are protected and remain on the substrate after development. In a negative photoresist, the exposed parts become insoluble and unexposed parts are soluble in the developer solution. After removal of the photoresist oxide layer is etched or it can be also used for deposition steps [4]. Photolithography process is used for patterning but there is a requirement of clean rooms and major cost is associated with the equipment making the process very costly and inconvenient [5].

2

1.1.2 Scanning Beam Lithography

Scanning beam lithography, also called as direct write lithographic techniques can be classified in two types; electron beam lithography (EBL) and focused ion beam lithography (FIB). Scanning beam techniques scans the surface of the substrate point-by point. This makes the process very slow and reduces throughput. As EBL takes more time in processing there is also vulnerability of beam drifting from its path. EBL has begun to find applications in direct writing, where the focused beam directly impinges on the resist which is sensitive to electron to pattern substrate. Considering the improved resolution of EBL, it is routinely used to generate master masks [6] and lines in the resist for submicron features.

In FIB the beam consists of ions which are scanned over the surface to be patterned. The ions may be used to initiate a chemical reaction on surface to be patterned or they may be directly sputtered. In FIB the ion scattering from the resist i.e. generally the surface to be patterned is very low. FIB is a maskless process although surface to be patterned could be damaged by the use of high energy ions [7]. Not only FIB is expensive but its throughput is also lower than with EBL due to difference in velocity of charged ions and electrons [8].

1.1.3 Soft Lithography

Soft lithography has been used to produce micron sized features on the substrate with advantages over conventional photolithographic techniques. Advantages include formation of micro structures patterned on nonplanar surfaces, fabrication of complex

3

optically functional surfaces, and fabrication of microelectronic devices [9]. Soft

lithography is based on pattern transfer using a mold for patterning the substrate material.

A master template is used for the mold formation used for patterning. Fig.1.2 explains the

mold preparation from master template. Printing is one form of soft lithographic

technique which has been broadly classified as

(a) Microcontact Printing

(b) Nanotransfer Printing
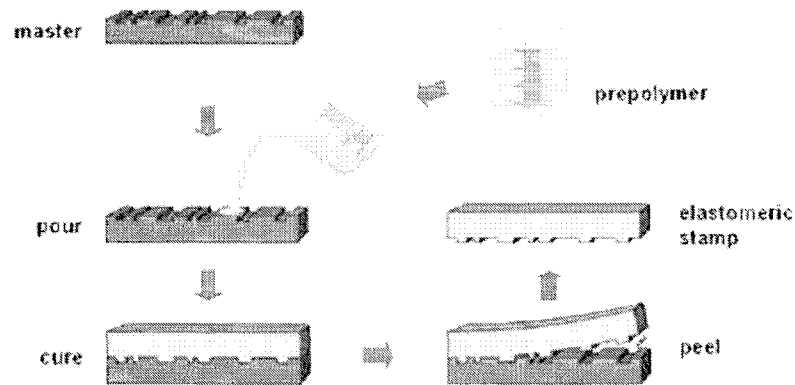
Fig 1.2 Mold formation by soft lithography [10]

Microcontact Printing - Whitesides and co-workers developed a technique called

Microcontact printing [11]. They have extended rubber stamping to replicate patterns

with features by the use of PDMS polydimethylsiloxane) and other elastomers. Desired

patterns can be created by the stamp that is inked with a material to be transferred. The

protruding features of the stamp are conformally contacted with the substrate to be

patterned. This stamp can be made by photolithography on which monolayer of organic

material can be patterned. After transferring the stamp's pattern onto the substrate,

different monolayer's can be formed on the stamped or the unstamped regions. One of the most significant advantages of microcontact printing over conventional photolithography is that it has the capability to form patterns on nonplanar surfaces [12]. Although it has advantage over lithographic techniques, wetting of the ink to get desired pattern plays an important role for good quality patterning.

Nanotransfer Printing - Nanotransfer printing (nTP) is an additive technique of printing micro and nanoscale features onto a substrate, without etching steps. Solid layer of material, typically metal, is used as 'ink' in this method. A elastomeric patterned stamp is coated with metal and it is transferred from the protruding features of the stamp. The substrate to be printed has an adhesion layer on its surface, designed to promote the adhesive bonding of the metal. The surface chemistries are used as interfacial glues and release layers to control the transfer of solid material coatings from the stamp to a substrate [13]. The strength of adhesion between the metal and the stamp is smaller than that of the substrate and metal during contact [14, 15].

Different surface patterning techniques discussed above have the limitation of many steps involved during patterning of a substrate with requirement of expensive equipment and controlled environment for processing. Lasers have advantage of high speed, spatial and temporal control, and a highly concentrated energy source whose properties such as wavelength, fluence, intensity, and polarization can be tailored in order to pattern a surface. In the next section laser based methods for patterning has been discussed.

1.2 Laser Based Techniques

Laser based patterning techniques have been developed and applied to deposit micron sized conductive lines for microelectronic applications such as mask repair or localized doping [16]. Among the laser patterning methods LCVD (Laser Chemical Vapour deposition) is most popular. Conventional surface patterning methods such as CVD and Plasma CVD cannot be location sensitive and selective precise patterning is also difficult to achieve. LENS (Laser engineered nano-shaping) is another such method which is recently gaining industrial interest.

1.2.1 Laser Chemical Vapour Deposition (LCVD)

LCVD is surface patterning technique for film growth where a continuous wave laser interacts with substrate in the presence of reactive molecules. The substrate is placed at the focal point of the laser beam in the chamber where the beam is incident perpendicular to the substrate surface. LCVD technique can be classified as photolytic and pyrolytic depending upon the method used to initiate chemical reaction with molecules in the reaction chamber shown in Fig 1.3.

The substrate is kept in vacuum before deposition of film. Then the chamber is pressurized to fill with a reactant gas. A stage is used in order to move the substrate in the chamber where the pattern is deposited and then the sample is evacuated. Certain prerequisites are required for a clean LCVD process such as stability of phase, vapour pressure etc. This process should also be carried out in controlled atmosphere such as in a

vacuum where the deposition rates are slow. Temperature control is essentially important for good quality deposition.

Laser Beam

Upper Reaction
Chamber

Reagent
Delivery Nozzle

Flexible
Bellows

Lower Chamber
Stage Housing

Thermal Imager
Port

Substrate

Resistance
Heater
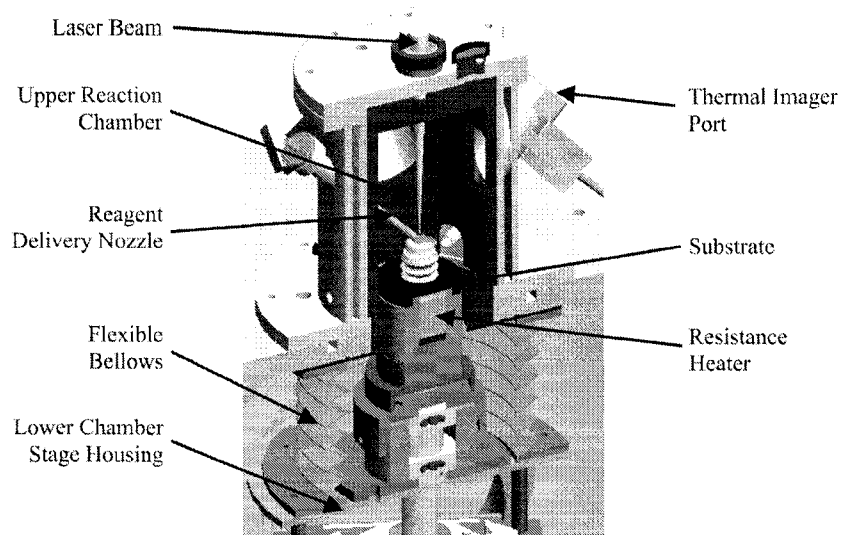
Fig 1.3 Schematic of the LCVD system [17]

1.2.2   Laser engineered nano-shaping (LENS)

Laser engineered nano-shaping (LENS) melts powders of various materials as the laser beam interacts with the surface of the substrate. In this process of interaction with the powder; the material melts and then resolidifies. During this transformation, the structural properties of the material would change resulting in residual stresses within the material. Limitations of this technique include overheating of the substrate and requirement of high power laser beams to pattern [18].

Other methods such as Matrix Assisted Pulsed Laser evaporation (MAPLE), MAPLE – Direct Write (MAPLE-DW), laser ablation transfer have the advantage that they are

"solvent" free deposition techniques, which allow depositing multilayer without the need to identify suitable solvent systems or to obtain a polymer that can be evaporated thermally. All of these techniques with the exception of MAPLE allow deposition with a "high" lateral resolution. MAPLE also involves use of a vacuum system making it an expensive choice.

Laser Induced Forward Transfer is also one such direct write technique which can be performed in the ambient conditions. However; for the simplicity of its technique and the ability to pattern metal features, LIFT offers advantage as a patterning technique for fabricating structures which is discussed further.

1.3   Laser Induced Forward Transfer (LIFT) – Direct Write Technique

Bohandy et al. discovered this method of direct writing in 1986 [19]. Metal features were ablated from a support that was optically transparent. This direct writing of metal features was done using excimer laser of wavelength 193nm. The depositions were made by single pulse. Laser-induced forward transfer (LIFT) is a direct-writing technique that allows patterning of different material with high amount of spatial resolution [20]. In this technique a small fraction of a solid thin film is vaporized by a laser pulse focused on the thin absorbing film through its transparent holder. Three stages in the process of LIFT are as follows:

- Removal of thin film from the donor substrate (DS)
- Transfer of the thin film under atmospheric pressure
- Deposition of film on acceptor substrate (AS)

8
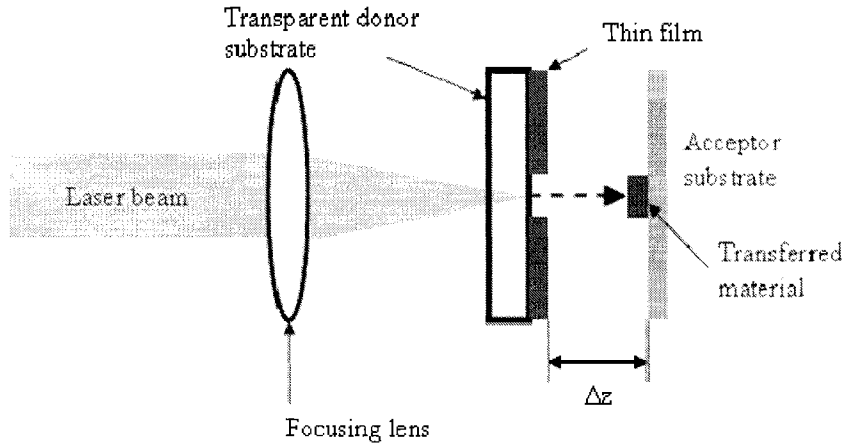
Fig 1.4 Schematic illustration of LIFT [21]

Fig1.4 shows the schematic diagram of LIFT for deposition of micron sized features where energy of the laser beam can be varied. Different materials require different amount of energy to ablate and deposit on AS. According to the literature there are two possible variations in the process of LIFT as discussed in the next section.

1.3.1   Front Transfer and Back Transfer

There can be two variations in the process of LIFT. It can be used either to front transfer the donor material or back transfer it [22]. In the conventional LIFT process of front transfer, a laser beam is focused through a transparent substrate on the thin film and film gets deposited on AS. In the process of back transfer the laser beam passes through the transparent acceptor and strikes on the free surface of the thin film which leads to its deposition on the transparent AS. Since the AS is transparent in back transfer LIFT; the DS in this process can be bulk material or even opaque. Fig 1.5 shows the schematic illustration of LIFT- front and back transfer.
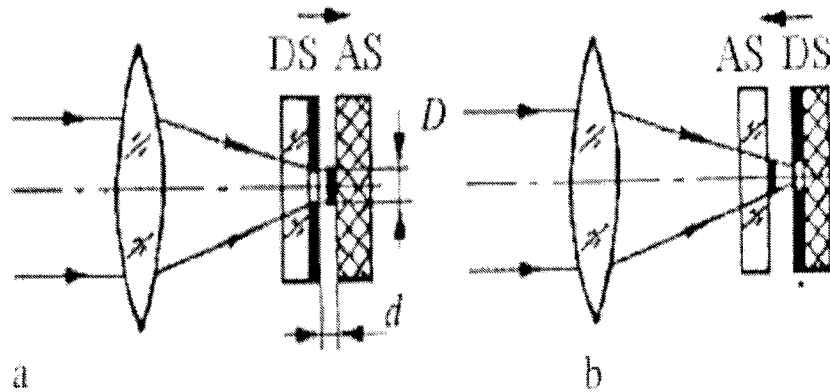
Fig 1.5 Schematic illustration of LIFT (a) front Transfer (b) back Transfer (AS is the acceptor substrate and DS is the donor substrate) [23]

1.3.2 Development of LIFT

LIFT was first introduced by Bohandy et.al in 1986 [19]. In 1987 work was further extended where Cu and Ag metal were deposited under vacuum pressure. They used an Nd:YAG laser, frequency doubled to 532nm, producing 10ns pulses for deposition [24]. The work suggested that deposition characteristics were same by 532nm as in case of 193nm. Best depositions can be obtained by using thinner films and lower laser power. However the exact reason for such deposition characteristics was given by Baseman et al. in 1988 [25] where they performed experiments on the donor film at higher and lower fluence. In their model partial evaporation of the donor films causes the film to propel as a mixture of gas and particles at higher fluence.

Fogarassy et al. (1989) deposited thin superconducting films by LIFT. Thermal analysis of film removal made in their study showed that the removal of thin superconducting

films take place only when its temperature is above its surface-melting threshold [26, 27]. Kantor et al. (1992) studied the effect of film transfer by varying film-to-substrate distance and also understanding the effect of adherence of film to the DS on the film transfer [28]. Thin films having good adherence to DS were compared with films having poor adherence with DS. Irregular ablation was observed for the films not adhering well to DS. They do not get deposited on the substrate since they cannot attain optimum temperature although complete ablation of the film would take place. In any case poorly adhered films showed no relation to film-to-substrate distance with its transfer yield. However for the range of 0 to 60μm; well adhering films showed clear film-to-substrate distance dependency. Deposition quality observed was good for distance less than 15μm (Δz as shown in Fig 1.4) between donor and acceptor and for fluence near the boiling point of the thin film.

Ultra short laser pulses mechanism in laser induced reverse transfer was performed by Bullock et al. (1997) using laser with pulse width in the order of 700 femtoseconds [29]. In this work of back ablation, velocity and the divergence of thin film of aluminum plume deposited on the substrate were evaluated. The glass substrate was placed at a distance of 1.63cm behind the aluminum film which was the target material. In order to study the plume behavior of thin aluminum films, Bullock et al. also worked on imaging technique such as shadowgraphs and time integrated photographs [30].

The LIFT process was performed with a femtosecond pulse laser by Zergioti et al. (1998) for depositing Chromium and Indium oxide on the glass and silicon acceptor substrate in

vacuum. Lines and dot patterns were serially written without much heat diffusion thus fabricating well defined features [31]. Yamada et al. (2002) did an optimization study of LIFT process where Nickel film which was deposited on silicon wafer of thickness 2.3mm. Nickel films of different thicknesses were used and KrF excimer laser ($\lambda \sim 248$ nm) with pulse width of 30ns for ablation. They revealed that laser spot size plays an important role in resolution of the deposited features [32]. In their case good quality deposition with clear edges was obtained when nickel film and silicon wafer were in close contact with each other. In their other work an experimental investigation revealed that when the fluence crosses the optimum value for deposition the pattern spreads on the AS due to thermal shock and that it spreads non linearly due at higher fluence[33].

P. Serra et al. (2004) have been working on transfer of biomolecules in liquid state by LIFT process. In their work arrays of DNA were transferred by this process. The transferred droplet volume displayed a linear dependence on the laser pulse energy. Controlled transfers of DNA patterns could be obtained by varying laser parameters [34-37]. Recent research work by Sudipta Bera et al. (2007) was regarding optimization study of LIFT process using thin aluminum film. In this work higher numerical apertures were found to deposit smallest features. Best features were obtained just above the printing threshold of the aluminum film. Threshold for pattern transfer was dependent on sample thickness, quality of focus, and pulse laser duration. Films of thicknesses 100nm and 500nm were deposited using femtosecond laser [38].

In the process of LIFT many different kind of laser systems have been used to pattern a surface. It is therefore important to understand the mechanism involved and the different parameters linked to this system which is discussed further.

1.4   Laser Mechanism

The word 'LASER' is originally an acronym for 'Light Amplification by Stimulated Emission of Radiation'. Population Inversion and Stimulated emission are two important concepts for the laser light to be emitted. Light is intensified by a process called stimulated emission by which laser can be generated. Stimulated emission is a special form of light interaction with material in atomic scale. In stimulated emission, the electric field of an incoming photon causes a molecule in a higher energy level to emit a photon of the same wavelength. In this process atom drops to a lower energy level. This photon which is stimulated will travel in the same direction as that of the original photon since they are in phase. The incoming photon is not affected in the process. A population inversion seen in Fig.1.6 is another necessary condition for the lasing process [39]. When the lasing medium is in equilibrium, the population of electrons at any energy state is determined by the Boltzmann equation. For a medium with two energy states, the relationship between energy and the electron population is given by equation 1.1.

$$N_2/N_1 = exp-(E_2-E_1/Kt) \hspace{3cm} (1.1)$$

Where N_1 and N_2 are the number of electrons at energy states E_1 and E_2 respectively, t is the absolute temperature of the medium, and K is the Boltzmann's constant. The goal of choosing a lasing medium and excitation methods is to induce a non-equilibrium state that contains more high energy state then lower energy state electrons. Under the

13

condition of the population inversion, sustained lasing action is possible because statistically more electrons are available to provide stimulated emissions than there are ground state electrons, which have the tendency to absorb the emitted photons.
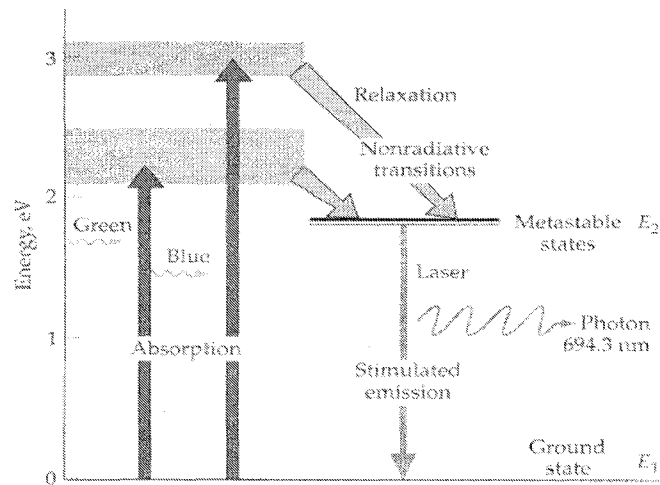
Fig 1.6 Illustration of population inversion process [39]

1.5 Laser processing parameters

In this process of LIFT, light interacts with surface to be patterned. This interaction depends on lot of aspects that include type of surface to be patterned, laser source used for patterning and many other parameters that are discussed below.

1.5.1 Temporal Profile

Laser beam emitted from the cavity of laser can be pulsed or continuous in nature. If the laser beam is continuously emitted, it is called continuous wave (CW) laser while the laser beam emitted with finite intervals or in a single shot, it is called a pulsed laser. The

time duration for which pulse laser is being emitted is the pulse width or pulse duration. The term repetition rate represents the frequency of such pulses [40] as shown in Fig1.7 Short pulsed lasers produce a small heat affected zone and a small recast layer on the machined surface by causing material vaporization through high peak power and shorter interaction time [41].
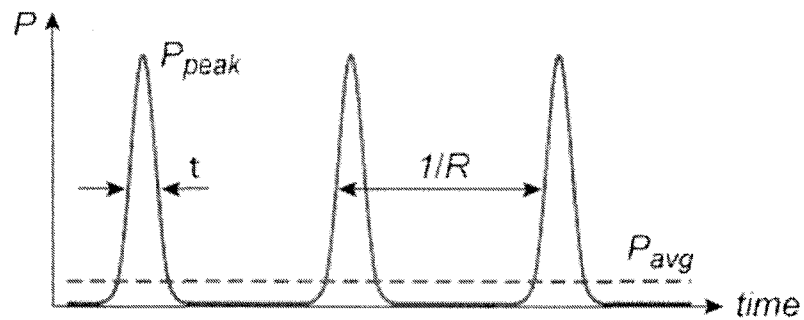
Fig 1.7 Temporal mode of pulsed lasers [44]

Where P is the power, t is the pulse width and R the repetition rate. In continuous wave and long pulse regimes the dominant process involved is the heating of the target material through the liquid phase to the vapor phase, resulting in expansion and expulsion of the desired target material [42]. This is accompanied by heating and collateral damage to the surrounding area, the degree of which is determined by the rate of energy absorption and the rate of energy loss through thermal conduction in the material [43]. This collateral damage is often detrimental and is a limiting factor when high precision ablation is required or when it may present a hazard, e.g. laser surgery.

1.5.2 Spatial Profile

In order to pattern a surface, the light must be focused to as small spot as possible. The size of the spot is determined by several factors, but the theoretical limit on the smallest feature that can be obtained is about the wavelength of the light. Spatial profile of spot defines how laser energy is distributed over the cross section of the beam. The most important and thoroughly analyzed profile is the Gaussian (or TEM00) mode. Fig 1.7 shows the Gaussian distribution of the laser beam. If, I is irradiance (W/cm^2), I_0 is the irradiance at the center of the beam, w is the radius of the beam waist where I drops to I_0/e^2.
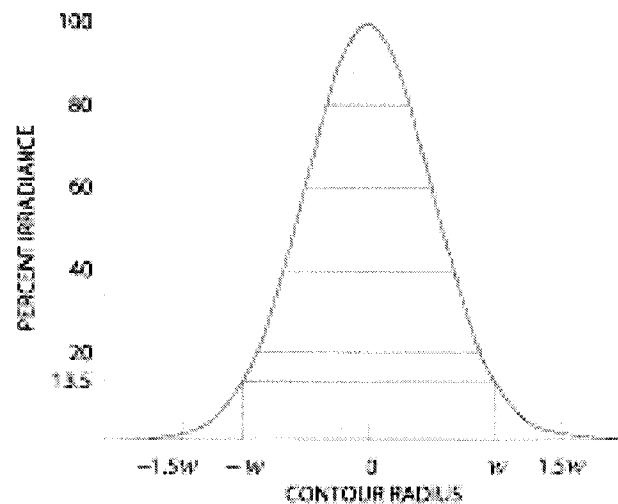
Fig 1.8 Gaussian beam profile [45]

1.5.3 Laser spot size and beam quality:

The quality of a laser beam can be defined in different ways but is measured by energy, its ability to focus, and its homogeneity [46]. If the beam is not of a controlled size, the laser-affected region may be larger than desired size with excessive slope in the

16

sidewalls. Laser spot size is the laser beam diameter at the focus. In order for the material to ablate the focus should be on the surface of the substrate. Generally the spot size is taken as Full Width Half Maximum (at 50 % irradiance) of the Gaussian profile as shown in Fig 1.8.

1.5.4 Peak power

Peak power generally is related to pulsed lasers. These laser systems are used in the process of LIFT now. There exists an optimum value of laser beam intensity such that the extremely localized material softening will occur. The peak power must be able to soften the work piece, but not strong enough to cause direct ablation. It is an instantaneous power available as an output to laser during the pulse time as shown in Fig 1.7 [47].

1.5.5 Pulse duration

Pulse duration is defined as the duration in which the laser pulse attains peak power. Theoretically, the pulse duration should not be longer than the thermal relaxation time for thermal diffusion in a target material. The short pulse duration can maximize peak power and minimize thermal diffusion to the surrounding bulk work material, leading to localized heating [47].

1.5.6 Pulse repetition rate

When the energy is sufficient, every pulse makes an effect on the target work piece. Repetition rate is the number of pulses hitting the target and it depends on the pulse duration. It determines the duty cycle while machining or deposition. If the repetition

rates were too low, lesser pulses would hit the target in given time reducing throughput while machining and vice versa. Also the thermal effects of material ablation would be less comparative to ablation at higher repetition rate [44].

1.6   Pulsed Laser – Micromachining Tool

Efficient use of lasers for precise material processing is impossible without a thorough knowledge of the fundamental laws governing the interaction of laser radiation with matter. The laser pulse duration plays a critical role in the laser material interaction, which, in turn, significantly affects the quality of the micro-feature created and also the material removal rate. Pulsed laser micromachining can be divided further based on thermal interaction with material. Pyrolytic process generally deals with micro and nanosecond pulses whereas photolytic process is based on femtosecond and picosecond lasers. In pyrolytic process chemical bonds in the target material are decomposed where as in photolytic process molecules of material absorbs energy to get into higher energy levels. For long energy deposition time's pyrolythic effect occurs causing degradation in patterning quality. Depending upon material system and the amount of energy used it is possible to use laser methods for patterning [48]. Based upon the material removal mechanism this discussion is divided in two parts.

1.6.1   Photolytic process

Generally femtosecond and picosecond lasers come under this classification. In order for the laser energy to get diffused in the target material some amount of time is required. This time is referred to as electron photon relaxation time and during this time electrons

18

of laser beam transfer their energy to target atom. The time is in the order of a fraction of a picosecond to several tens of picoseconds [49]. Since the electron relaxation time is negligible in photolytic process, less heat dissipates through the material to be processed. Femtosecond pulsed laser is a rapidly advancing area of ultrashort laser applications. Much of the research is carried out in the field of patterning with femtosecond laser pulses.

It utilizes the ultrashort laser pulse properties to achieve high degree of control in patterning desired microstructures without collateral damage to the surroundings [50]. Since the pulse period is so small; laser energy is deposited at a time scale much shorter than both the heat transport and the electron-phonon coupling, the light-matter interaction process is virtually negligible. Due to these reasons very small feature sizes can be obtained the dimensions of patterns or machining features can go beyond wavelength of the light [51]. In picosecond laser ablation, pulses are of the same time scale that it takes to transfer energy from electron to the lattice of the material being machined. There is little heat conduction but a great deal of heat flow caused by free electrons. At the surface, there is a solid-to-plasma phase; however, there is a liquid phase "inside" the material.

Industrial applications of femtosecond lasers are still not clear and with the laser system being very expensive. However, rapid developments in other solid-state lasers continue to extend the frontiers of high quality laser micromachining using nanosecond pulses [52]. The material removal mechanism is pyrolytic in nature for such lasers.

1.6.2 Pyrolytic process

Laser pulses in nanosecond regime have shown the ability to pattern wide variety of materials where the ablative mechanism is pyrolytic in nature. The patterns were fabricated with micron size precision with sub micron size recast layers. The material modifications begin with its melting followed by its ablation. Comparisons in literature show intrinsic differences in the quality of machining based on pulse format alone which can give misleading impression. Also nanosecond lasers are cost effective and easily available and have greater industrial interest than femtosecond lasers which still is only in the level of research.

1.7 Structured Patterning – Applications

Ablation of thin metals and organic substrates is an attractive method of generating precisely defined features in many types' miniaturized components in the field of electronics. Complex photolithographic steps can be avoided in order to gain high end productivity at high throughputs. One such application is to pattern lines of gold on a flex substrate by ablation using excimer laser. The length of the patterns is about $200\,\mu m$ and there has to be variation in the width as seen in Fig 1.9. The thickness of these patterns may vary from 100 to 500nm. In order to pattern such substrates masks have to be used and the illuminating laser beam has to be fully homogenized and shaped in order to create uniform patterns.

Another such application in the field of microelectronics where the gold interconnects lines patterned on PDMS substrate as shown in Fig 1.10. Such a device finds grater

application in the biological field to trap a particle. Standard photolithography was adopted in creating fluidic channels that were 40μm wide and 10μm high with 200μm spacing. In order to pattern gold electrodes on top of these fluidic channels, lift-off was performed using a very thick resist.
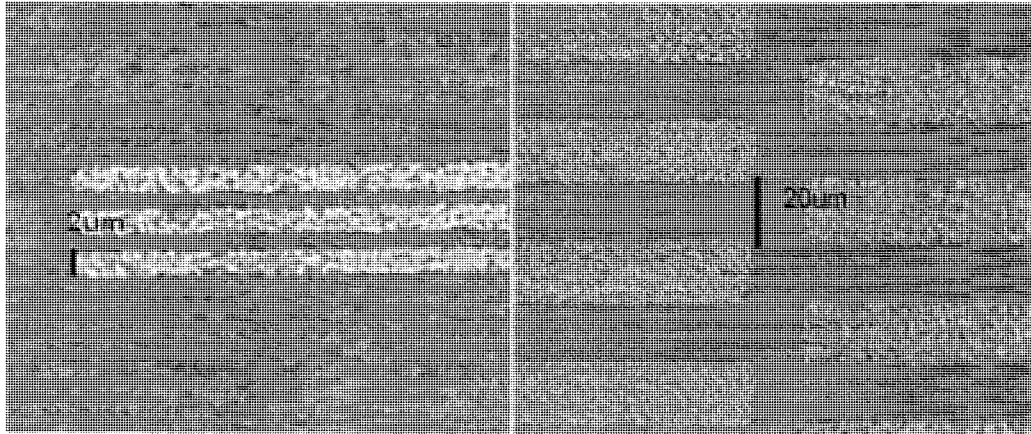
Fig 1.9 Gold Patterns on Flex substrate [53]

Conformal coatings of such line patterns find good biomedical applications in catheter tubes and stents. Such devices require radioopaqe biocompatible coatings which do not wear out easily and are corrosion resistant. The thickness of such coating is in the order of nm to μm with varied spacing between them. Fig 1.11 shows an electrode prepared by deposition on catheter tube with bands of radioopaqe coating.

Such structured multiple line patterns are important from applications point of view finding its requirement in branches ranging from electronics to biology. However the number of steps involved in its manufacture makes the process more complex and expensive. LIFT with the process of laser beam interference has been used in few works

21

discussed later in this section, to structure multiple dot arrays on a substrate. Interference of laser beam briefly discussed further would make the process of such structured patterning much simple.
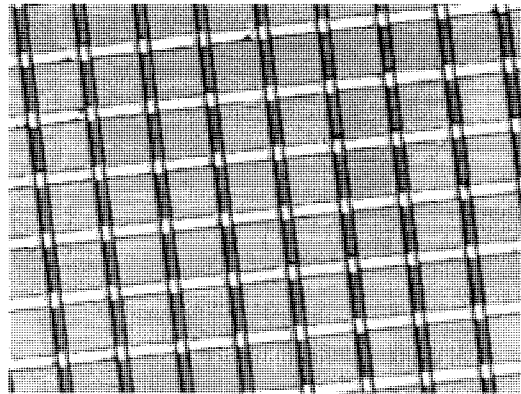
Fig 1.10 Gold interconnects on PDMS substrate [54]
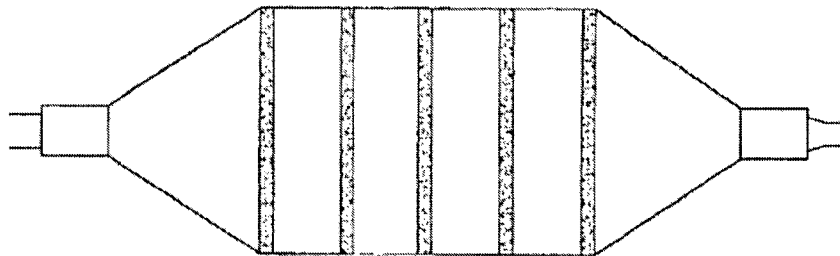
Fig 1.11 Schematic illustration bands of radioopaqe coatings [55]

1.8   Interference

If two or more light waves of same frequency overlap at a point, the resultant effect depends on the phases of the waves as well as their amplitudes. The resultant wave at any point any instant of time is governed by the principle of superposition. The combined effects at each point of the region of superposition are obtained by adding algebraically

22

the amplitudes of the individual waves [56]. The point where the amplitudes add up is called as the constructive interference while if they cancel out it is called destructive interference. In a bright and dark bands obtained by interference of two light waves; all the bands are called as interference fringes. Thus the phenomenon by which the energy of light is redistributed due to superposition of light waves from two or more sources that coherent in nature is called as interference. In order for the light waves to interfere it must fulfill some conditions and also to get a well defined pattern.

1. The light waves should be of the same frequency

2. The light waves must be coherent

3. Path difference between the two waves must be less than the coherence length of the light
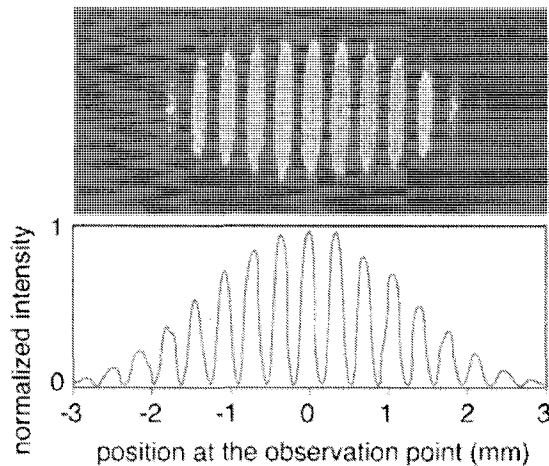
Fig 1.12 Interference patterns formed by interference of two laser beams [57]

Fig 1.11 shows the pattern formation by the interference of the two laser beams. This light pattern is simply the variation in intensity and thus the amplitude of the two light

waves caused by its superposition discussed earlier in this section. The bright bands refer to regions where the normalized intensity is maximum Fig 1.12 and dark bands refer to regions where its intensity drops to zero.

1.8.1   Interference in Surface Patterning

D. Bäuerle et al. (2005) demonstrated surface patterning by means of regular two-dimensional (2D) lattices of microlenses for large number of various different systems by interference. As the laser beam passes through the substrate with microsphere, each microsphere acts as a microlens which focuses the laser radiation onto the substrate [58]. These microlenses cause the beam to interfere thus patterning the substrate with dots.

There are few studies on the incorporation of interference phenomenon in femtosecond laser interference micromachining. Kawamura et al. (2001) introduced a two-beam holographic method to encode surface relief and sub-surface micro gratings [59, 60]. Similar concept was found in the setup proposed by Zhai et al. (2001) for the fabrication of gratings in bulk polymer medium [61]. Oi et al. also proposed a fabrication technique for Giber Bragg gratings by femtosecond laser interferometry [62]. In all the above-mentioned set-ups, a femtosecond pulse was split into two beams, and then overlapped again on the desired surface to generate a linear interference pattern. As a result, gratings were formed with a periodic peak/valley structure that corresponds to the dark/bright linear interference fringes.

1.8.2 Interference in Laser Induced forward Transfer

In the literature two attempts were found for patterning substrate by combining interference and LIFT process however both attempts were to fabricate only dot structures. Until now, there has been no emphasis on regular and longer dimensional patterns by LIFT and interference. Since laser-induced forward transfer (LIFT) technique has been extensively studied for micro printing diffractive optical structures and computer-generated holograms, writing active and passive mesoscopic circuit elements and arranging pad array in microelectronic packaging etc., it would be very appropriate to have longer dimension patterns for varied applications. Quan-Zhong Zhao et al. (2005) implemented optical interference method for transferring periodic microstructures of metal film from a supporting substrate to a receiving substrate by means of five-beam interference of femtosecond laser pulses [63]. The periodic structures were dot arrays with a period of 2.5μm on both acceptor and donor substrate. The optical setup used was similar to Fig 1.13 where DBS is the diffractive beam splitter; L1 and L2 are the lenses and AA is the aperture array [64].
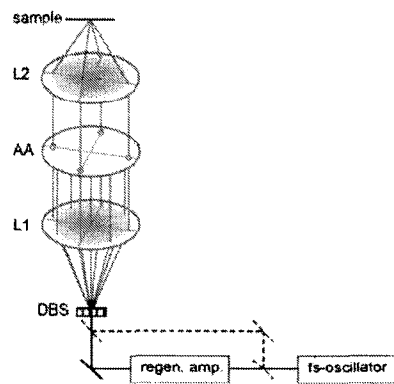
Fig 1.13 Setup for fabrication of periodic structure by femtosecond laser interference

[64]

25

Fig 1.14 (a and c) show the optical microscope an SEM images of dot structures on donor substrate while (b and d) are similar images on acceptor substrate respectively. The material was thin Aluminum film that was deposited on transparent quartz plate and donor was quartz glass substrate.
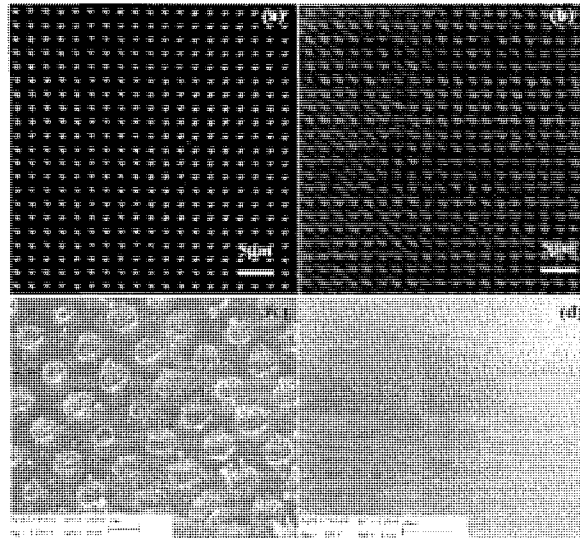
Fig 1.14 Dot array on quartz glass substrate [63]

In another work as shown in Fig 1.15 solid-phase deposition by laser-induced forward transfer (LIFT) has been performed by using thin metal foils in close contact between the microspheres and the substrate. By this means, hexagonal patterns of metal dots on arbitrary substrate materials together with the corresponding holes in the metal foils have been produced by single-shot KrF-laser irradiation by Landström et al. (2004) [65]. Patterns of gold thin film on regular two-dimensional lattices of microspheres that was used for patterning arrays of gold dots on different substrates as well as well-defined apertures on the surface of the microspheres. Also aluminum dots were deposited on

26

quartz in dot arrays. The size of the dot was $6\,\mu m$ where films with thicknesses of either

50 nm or 100 nm were employed for fabrication of such mask.
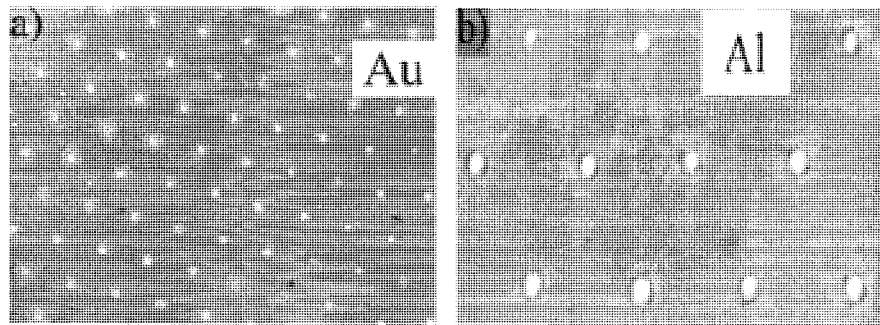
Fig 1.15 Hexago*nal lattice (a) gold dots and (b) aluminum dots [65]*

1.9   Motivation for this work

LIFT is the process by which thin films of metal, semiconductors, oxides, and

superconductors and also liquids can be transferred onto a substrate. The process can take

place under ambient conditions and does not require additional equipment for vacuum

thus making this process of patterning very cost effective. Some modification in this

technique can also result in complex deposition of liquids, pastes, inks and even

biological organic solvent. However the basic ideology behind the technique remains the

same. This technique is repetitive in nature and similar results could be obtained time and

over by adjusting proper experimental parameters. LIFT has been studied for many years

and the work previously done motivates us to select this method for patterning owing to

its industrial advantage as well. The work deals with deposition of line patterns of thin

gold film on the glass substrate by $Nd:YVO_4$ (Neodymium Doped Yttrium Vanadate)

laser interference having central wavelength of 1064nm and pulse width of 14ns.

27

1.10   Objective and Scope

Objective of this work is to patterns line features combining LIFT and nanosecond laser interference by an optical setup that is easy to manipulate. In order to accomplish this, the scope of this work includes.

1. Analysis of the LIFT and optical interference for depositing line patterned structures

2. Theoretical modeling to evaluate the dimensions of the deposited patterns by LIFT

    2.1. Due to the influence of laser parameters

    2.2. Due to the influence of optical setup parameters

3. Configuring the optical setup for interference assisted patterning

1.11   Summary

Biomedical and microelectronic devices require structural patterning for its functional application. Although many techniques are available for such patterning, these techniques are cumbersome and process oriented. Direct write technique known as Laser Induced Forward Transfer is a simple technique for patterning a substrate surface in ambient conditions. So far, LIFT has been used for patterning dot structures using interference. Patterning has been done either sequentially and no emphasis is laid on multiple lines patterning in single shot. LIFT technique combined with laser interference will serve as an alternative to the existing patterning techniques in the market. With the help of this method line patterns can be created efficiently and with simple modification in the setup its dimensions can be modified.

CHAPTER 2   PREDICTIVE MODELING

2.1   Introduction

As discussed in literature review the objective of this work is to introduce interference in the process of LIFT to selectively create and modify line patterns. Since laser is the tool by which this modification should be achieved; it is important to understand its interaction with material.

2.2   Nanosecond laser material removal

Nanosecond lasers interact thermally with any material. In this interaction thermal wave is propagated within the material and energy of each nanosecond pulse is absorbed by material. This absorbed energy first heats the surface of the material to its melting point and then to its vaporization temperature. Conduction within the material itself is the main cause for the loss of energy during this interaction. Especially in the case of metals much energy is required to vaporize than to melt which influences the ablation depth [66]. The ablation depth per pulse in nanosecond regime is given by equation below.

$$Z_a \approx \sqrt{(at)} \, Ln \, [F_a/F_{th}] \tag{2.1}$$

Where Z_a is the ablation depth, F_a is the absorbed energy, F_{th} is the threshold energy, and (a.t) is the thermal diffusion depth. F_a depends on the amount of energy available at the surface of the material within the focused laser spot. Consider a beam coming from the laser having diameter 'D'. This beam needs to be focused onto the target material in order to ablate with least power possible. Using a lens with focal length 'F', the beam coming from the laser is focused on target material where it interacts with the material. In this

focal region the laser beam is effective for a certain range for material removal along its

axis. The profile of the focused beam along its axis of propagation (z) is shown in Fig 2.1

2.2.1 Spot Size

Focal spot size represents an ultimate limit that is set by diffraction of laser beam and

applies only if the spatial distribution in the beam is Gaussian in nature.
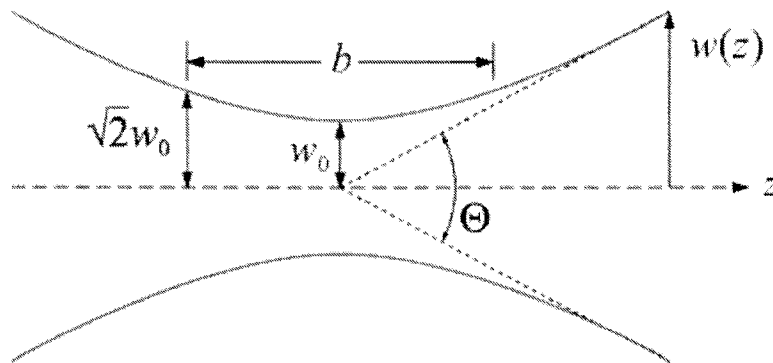
Fig 2.1 Geometry of a focused Gaussian beam along its propagation axis [67]

As seen in the Fig 2.1 geometry of the focused Gaussian beam has certain beam

parameters. The beam spot size w(z) will be at a minimum value w_0 at one place along

the beam axis, known as the beam waist. For a beam of wavelength λ at a distance z

along the beam from the beam waist, the variation of the spot size is given by equation

2.2.

$$\int w(z) = w_0 \sqrt{1 + \frac{z}{z_R}} \qquad (2.2)$$

Where, z_R is known as Rayleigh range and this range sets the range for effective machining 'b' of the material along the depth of focus of Gaussian beam given by equation 2.3.

$$b = 2 * z_R \qquad (2.3)$$

The transverse intensity distribution at every point along this range will be according to Fig 1.8 discussed in literature review and will vary along this range. For nanosecond lasers, since the threshold for the ablation of a material is not clearly defined, the spot size of a Gaussian beam is considered as the distance across the center of the beam for which the intensity equals $1/e^2$ of the maximum intensity as shown in Fig 1.8. This focused beam will contain 86.5% of the total energy (or power) of the Gaussian beam [68]. Along the Rayleigh range minimum diameter of the focused laser beam spot having waist radius w_0 given by the equation 2.5 below in terms of beam divergence angle (θ) [69].

$$\theta = 2.44\lambda/\Pi w_o \qquad (2.4)$$

When a focusing lens having the focal length 'F' is used to focus laser beam having divergence as given in equation 2.5; the spot size can be calculated as

$$Spot\ Size = \theta *F \qquad (2.5)$$

In this work interference patterns need to be created at this focused spot with the help of two laser beams. To create this interference pattern as shown in Fig 1.11; two laser beams having similar polarization should be superimposed at the same point on the surface of the material. This is same as interference of two plane waves travelling in same direction. Consider two plane waves u_1 and u_2 with propagation direction n_1 and n_2 that lie in the xz-

31

plane making the angles θ_1 and θ_2 to the z-axis; α = the angle between n1 and n2, θ = the

angle between the line bisecting α and the z-axis as shown in Fig 2.2.
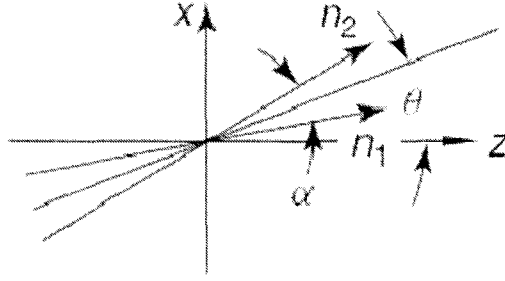
Fig 2.2 Interference of two plane waves [70]

The complex amplitude of the two plane waves is given by following equations.

$$u_1 = U_1 e^{i\varphi 1} \tag{2.6}$$

$$u_2 = U_2 e^{i\varphi 2} \tag{2.7}$$

where,

$$\phi_1 = k\left[x\sin\left(\theta - \frac{\alpha}{2}\right) + z\cos\left(\theta - \frac{\alpha}{2}\right)\right] \tag{2.8}$$

$$\phi_2 = k\left[x\sin\left(\theta + \frac{\alpha}{2}\right) + z\cos\left(\theta + \frac{\alpha}{2}\right)\right] \tag{2.9}$$

And with the general equation given as

$$\Delta\phi = \phi_1 - \phi_2 = k\left\{ x\left[\sin\left(\theta - \frac{\alpha}{2}\right) - \sin\left(\theta + \frac{\alpha}{2}\right)\right] + z\left[\cos\left(\theta - \frac{\alpha}{2}\right) - \cos\left(\theta + \frac{\alpha}{2}\right)\right]\right\}$$

$$= 2k\sin\frac{\alpha}{2}\left\{ -x\cos\theta + z\sin\theta\right\} \tag{2.10}$$

equation 2.9 is can be compared to the real part of the plane wave equation falling

obliquely on to a plane parallel to it at a particular distance given by equation 2.11.

32

$$u = Ue^{ik(x\sin\theta + z\cos\theta)} \tag{2.11}$$

And the distance between the interference fringes is given by equation 2.12

$$d = \frac{\lambda}{2 * \sin\alpha} \tag{2.12}$$

The intensity distribution is thus calculated by substituting z=0 in equation 2.10 leading to equation 2.13 [70].

$$I = I_1 + I_2 + 2(I_1 I_2)^{1/2} \cos(\varphi) \tag{2.13}$$

Where I_1 and I_2 are the intensities due to the two waves acting separately, and $\varphi = \varphi 1 - \varphi 2$ is the phase difference between them. Maximum and minimum intensities are dependent on the phase difference between the two waves varying from 0 to 180^0 respectively and considering $I_1 = I_2$. Thus $I_{max} = 4I$ and $I_{min} = 0$.

Maximum and minimum intensities at the interference focal point decide the visibility of interfered waves at a point. Visibility of such interference pattern is given by equation 2.13

$$V = \frac{(I\max - I\min)}{(I\max + I\min)} \tag{2.14}$$

For better contrast in the interference patterns (V should be = 1) two conditions must be satisfied distinctly.

- Intensities of both the interfering waves should be equal, $I_1 = I_2$

- The two interfering waves should have path difference (PD) < coherence length L_C of the laser.

Theoretical modeling has been done to show the difference in the beam profile by incorporating interference of Gaussian beam as shown in Fig 2.3.
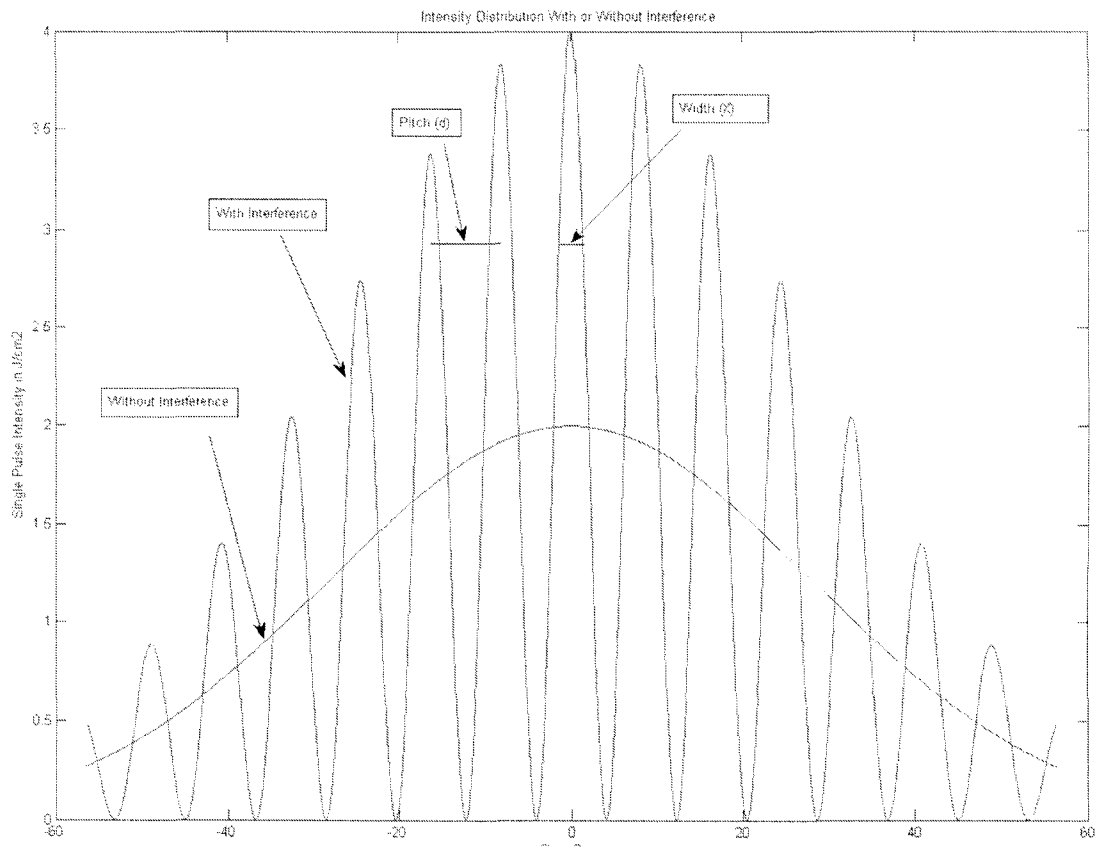
Fig 2.3 Comparison of Intensity distribution of interfered beam with non interfered beam

profile

The x- axis in Fig 2.3 denotes the size of the laser focused spot and y-axis the intensity. The line patterns as shown in Fig 1.12 are also called as fringes in interference patterns. The distance between these lines is given by equation 2.12. In order to vary the line patterns by LIFT process the two laser beams have to interfere at the interface of the donor substrate and thin film. The possible variation in these patterns can be done by

34

changing the width (X) of the line or by changing the distance between the lines known as pitch (d) as seen in Fig 2.3. Width can be changed by modifying laser whereas the pitch can be modified by optical parameters in the setup.

Predictive modeling has been done to identify the optimal laser and setup parameters. This modeling was divided in two separate parts. First part of the modeling deals with the optical setup parameters. There are two aspects considered while making the predictive model for variation in laser and optical setup parameters. Variation in pitch i.e. the distance between the two fringes created by interference at the focal plane due to change in the angle between the two interfering beams has also been predicted. The mathematical simulation has been supported by basic theory in its relation. In the second part, modeling has been done to study the effect of DS thickness in LIFT process for fringe pattern variation.

Modeling was performed for the following considerations. A 14 nanosecond pulse width laser system having wavelength=1064nm has a tunable repetition rate from 20 to 100 kHz. Gold film (thickness=50nm) ablated from the glass DS (thickness=3mm) is deposited on glass AS. Chromium film (thickness=5nm) is coated on Glass DS before the gold film is sputtered on to it to ensure good interfacial adherence with DS.

2.3   Modeling of Patterns ablated at different energies

In nanosecond regime the ablation threshold of the material is not clearly defined since in this regime the process of ablation takes place by thermal mechanism. However an

estimation of variation in fringe patterns with respect to pulse power will allow us to optimize laser parameters for good quality deposition. At 1064nm Chromium has threshold fluence of 1.5 J/cm^2 [71]. For this reason we can predict that at low fluence the chromium will ablate from the DS enabling gold to get deposited on AS. In this case the laser beam is incident at varied angles at the interface of DS and film. The value of threshold will also change accordingly. In this mathematical modeling the effect of laser pulse energy on number of fringe patterns ablated is shown in Fig 2.4
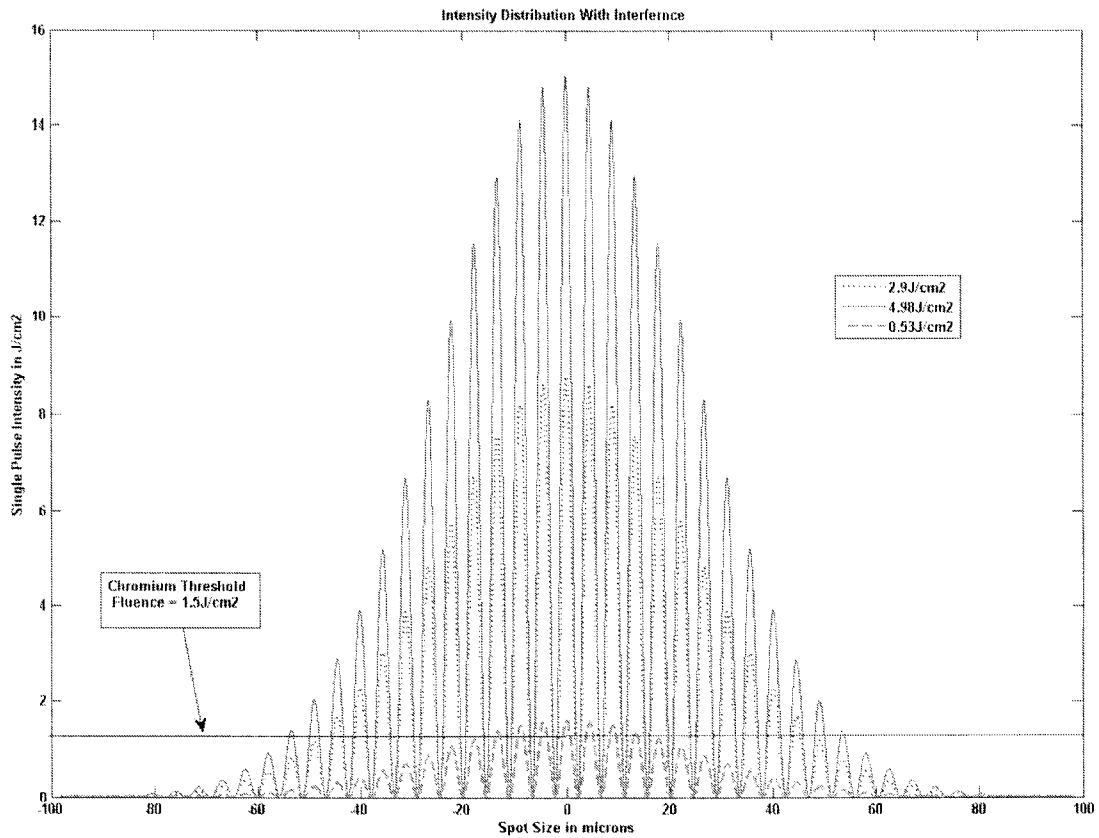
Fig 2.4 Interfered beams interference patterns at varied laser fluence

Fig 2.4 shows fringe pattern ablation at 0.53, 2.9, and 4.98J/cm^2 respectively. From the figure it can be predicted that with increase in energy, the area of ablated spot size increases. This can be attributed to change in Gaussian intensity distribution within focused region. Fig 2.5 shows the method to measure the size of the focused spot i.e. the region above threshold fluence. As seen in the figure for the fluence of 2.03J/cm^2 the focused spot size is 73 μm. From the figure it can also be predicted that with increase in the pulse power the ablated fringe width also increases.
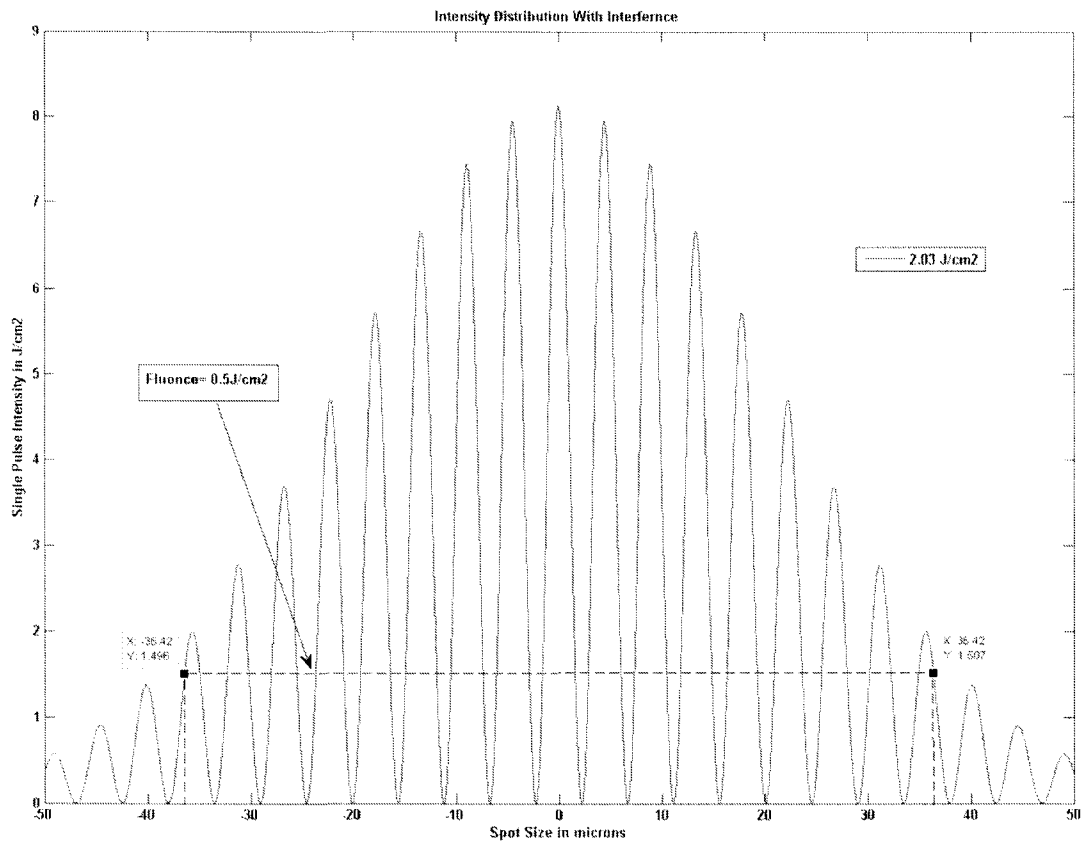
Fig 2.5 Measuring length of the focal spot

Finally it can be predicted from this part of modeling that the number of fringe patterns as well as feature size of each fringe pattern increases with increase in energy.

2.4   Variation in pitch

Modeling has been done to predict variation in pitch of the fringe patterns considering the optical setup planned for this work. The setup was modified from the literature [72]. As per the setup selected for this work variation in the pitch as well as feature size of each fringe pattern can be changed by changing the angle between the two interfering beams. Relationship between the pitch and the angle between the two beams given by the equation 2.12, is discussed in this section.
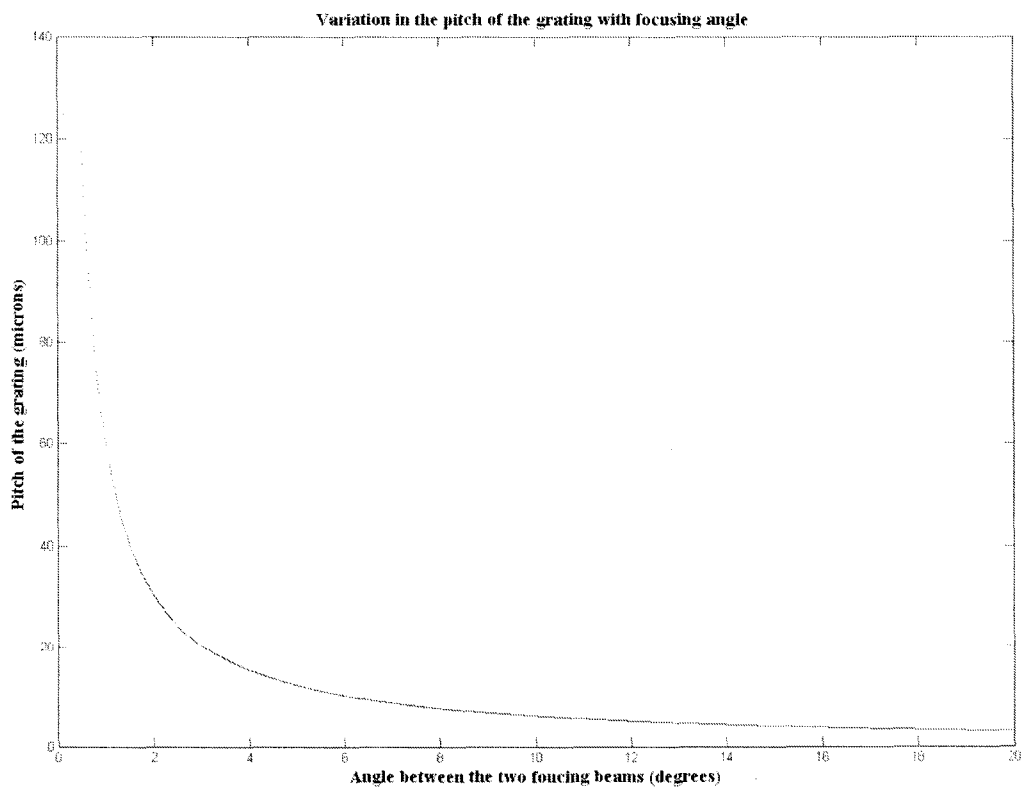
Fig 2.6 Pitch Variation due to change in the angle between two interfering beams

38

It can be predicted from Fig 2.6 that the pitch between the fringe patterns can be increased by decreasing the angle between the interfering beams and vice versa. For higher focal length lens the pitch will be more as compared to the lens having lesser focusing distance. But as the angle increases above 10^0 the variation in the pitch is negligible. The angle between the interfering beams also depends on the thickness of the DS as well as its refractive index discussed below.

2.5   Variation in Spot size due to donor substrate

The LIFT technique uses Donor substrate, Acceptor Substrate and a thin film. The laser beams should be focused at the interface of DS and the thin absorbing film to create interference patterns. As the laser beam passes through the donor substrate first there will be associated variation in laser spot size due to change in the refractive index of the medium from air to DS material. Possible variations due to this are taken into account for effective transfer of patterns by LIFT. The modified patterns in turn will get deposited on the acceptor substrate that is to be patterned. In Fig 2.6, n1 and n2 denote the refractive index of air and glass substrate respectively. θi is the angle of incidence and θr is the angle of refraction of the laser beam to the normal of the DS.

It can be seen in the figure that the refractive index of the DS of thickness (t) will play significant role in changing the spot size of the interfered beam. In the first case where n1=n2 there will be no variation in the spot size. Also the thickness of DS would not affect the spot size. However when the refractive index of the DS n2 > n1 there essentially will be difference in spot size. The thickness of the DS would also play an

39

important role in changing the size of the focused spot. For the mathematical modeling, refractive index of glass (n2=1.54) and air (n1=1) has been considered for the glass thickness of 3mm. Variation in the focused spot size is well explained with the help of Fig 2.7.
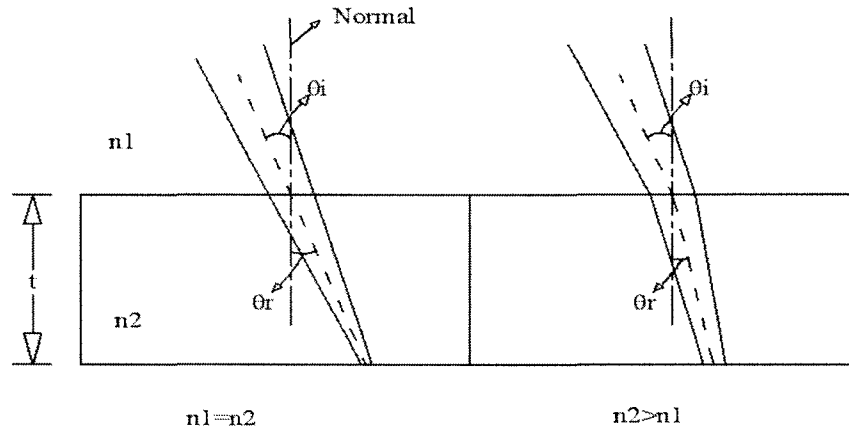
Fig 2.7 Variation in spot size due to refractive index of donor substrate

From the Fig 2.8 it can be said that there will be significant increase in the focused spot size due to the refractive index of the donor substrate for higher DS thickness. Increase in the spot size due to refractive index varies with respect to focusing length. Variation in the spot size is due to the limiting angle to which laser beam can be focused on the surface of the donor. At lower focal lengths the variation in spot size increases. The variation in the spot size would also be attributed to the thickness of the substrate itself. Lesser is the thickness of the substrate lesser would be the variation. As seen in the above figure the change in the spot size varies linearly with lenses having focal lengths above 20mm, however below this the variation is non linear. It is also evident that smaller features can be ablated from the DS by using lenses of lower focal length. In order to

40

optimize between non linearity and smaller features, experiments can be done with lenses having focal length F=50mm and above.
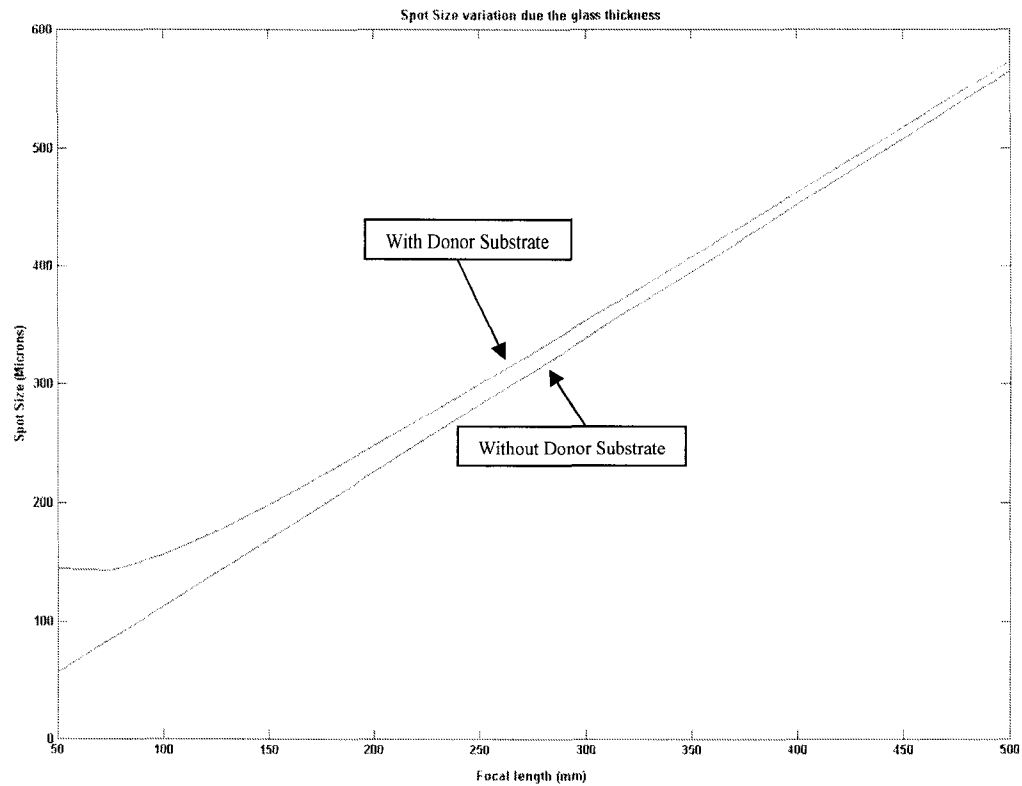
Fig 2.8 Spot Variation due to refractive index variation of donor substrate

2.6 Estimation of force to ablate gold film of varying thickness

In case of nanosecond regime the ablation process is explosive in nature. During this process of ablation in LIFT two dominant forces are considered responsible for the process of film removal [73]. First is the vapor force (F1) and second is the shearing force (F2). Equations 2.14 and 2.15 correspond to vapor force and shearing force respectively.

41

$$F1 = Spot\ Area\ *P \qquad\qquad (2.14)$$

$$F2 = Perimeter\ of\ Spot*t*\ shear\ stress \qquad\qquad (2.15)$$

Where, P is the vapor pressure and t is the thickness of gold film. It is considered that as the width of the laser spot decreases the F2 becomes dominant in film removal process and the ablation happens only due to shearing action. Fig 2.8 shows that the shearing force varies linearly with film thickness. From the above figure, it can be predicted that with increase in film thickness the force necessary to ablate the gold film also increases.

Variation in the Force required with film thickness
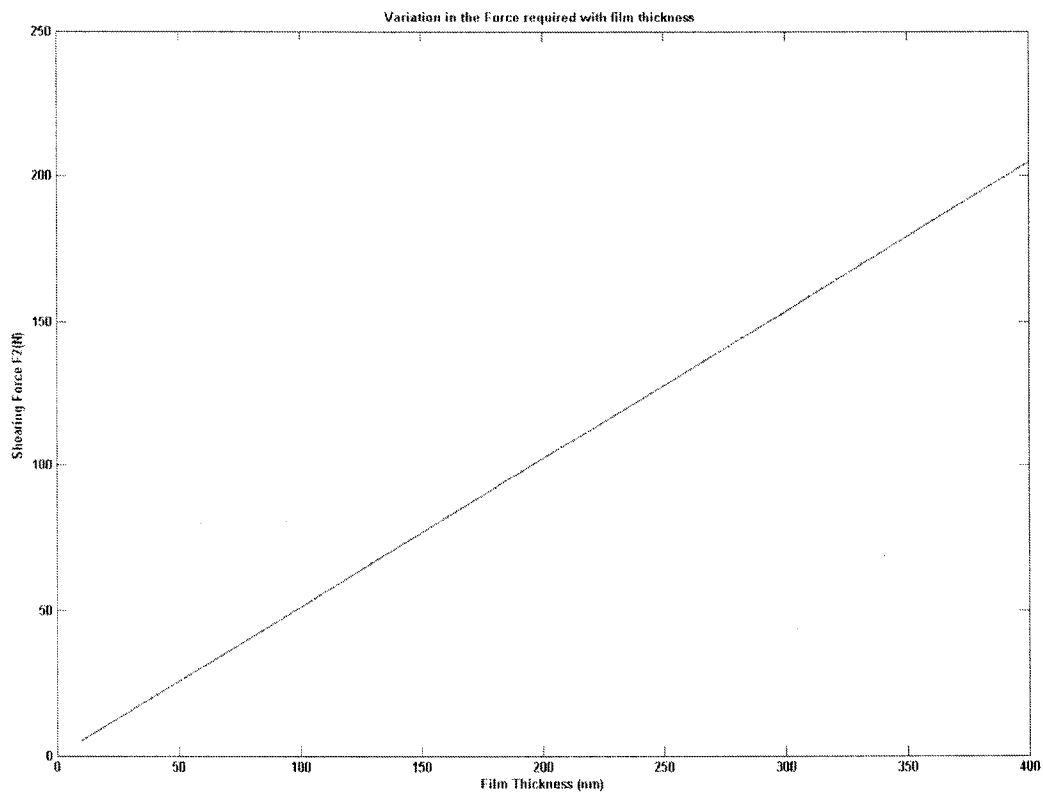
Fig 2.9 Shearing Force variation with film thickness

2.7   Summary

Predictive modeling has been done to optimize the optical and the laser parameters. Effect of different laser parameters on the dimension of the patters to be ablated from the DS is predicted. From the modeling it is also clear that optical parameters of the setup such as focal length of the lens and the distance between two parallel beams made to interfere play an important role in deciding the dimensions of the pattern to be deposited. The thickness and the refractive index of the DS will affect the effective laser spot diameter at the interface of DS and thin film thus creating difference in the line patterns deposited on the substrate.

CHAPTER 3   EXPERIMENTAL SETUP

3.1   Introduction

The objective of depositing line patterns by setting up the proposed optical configuration has been discussed in this section. With the proposed configuration, line patterns can be formed and the dimensions modified by varying the interference fringes formed at the focal plane i.e. at the interface of glass and gold film. Some minor modifications have been introduced in the optical setup from the previous work [74]. These modifications are done to change the distance between the two parallel beams before interference. Experimental setup on the whole has been divided in three sections which are discussed in this section. Sample preparation was the initial step before starting the optical setup is discussed further.

3.2   Target Sample

Samples on which experiments were done were simultaneously prepared while setting up the optical configuration. The donor gold film in experimental study was deposited on a 3mm glass substrate by conventional process of magnetron sputtering. Magnetron Sputtering is one form of physical vapor deposition technique which allows greater functionality, as thicker films can be produced in comparison to other surface coating techniques [75]. Glass is mechanically robust, optically transparent, biocompatible material. It is chemically resistant and electrically isolated. Owing to its properties it has found applications in the field of bioMEMS for producing biochips and microinjectors [76, 77]. Hence glass was selected as the acceptor substrate as well as the donor substrate

as it is also economical and widely available. Samples with gold film thicknesses of 50nm, 100nm and 200nm were coated to study the effect of power required to ablate the different thickness thin film on glass donor. The donor substrate with 50nm gold thickness was obtained from photonic Inc. while the other donor samples were custom made. Thickness all the samples was measured using optical profilometer. A chrome layer of 3 to 5 nm was first sputtered on the donor glass substrate so as to have good adherence with the sputtered gold film. The glass acceptor substrate (thickness=1mm) was kept in close contact to the donor substrate with the help of clips. Acceptor substrate, donor substrate and thin absorbing film make up the target for the experiments in this work. Fig 3.1 shows the target used for the experiments.
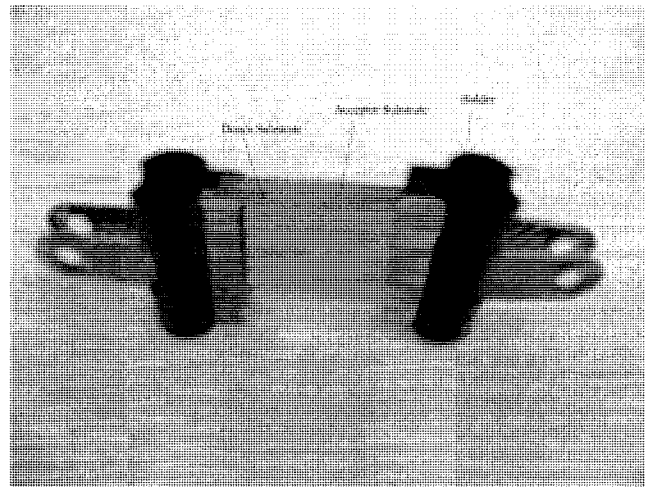
Fig 3.1 Target for depositing line patterns in the setup

3.3   Alignment of the optical configuration

The optical setup selected for experiments had some challenges while physically setting up the whole configuration. Initially the laser head was adjusted to appropriate height on

the vibration isolation table by which height of other optical devices could be manipulated later on while setting up the configuration. The laser beam was regularly monitored by infrared card, since the laser beam was invisible owing to its wavelength thus preventing any deviation in laser beam path. Few challenges faced during the setup shown in Fig 3.2, have been discussed in detail.
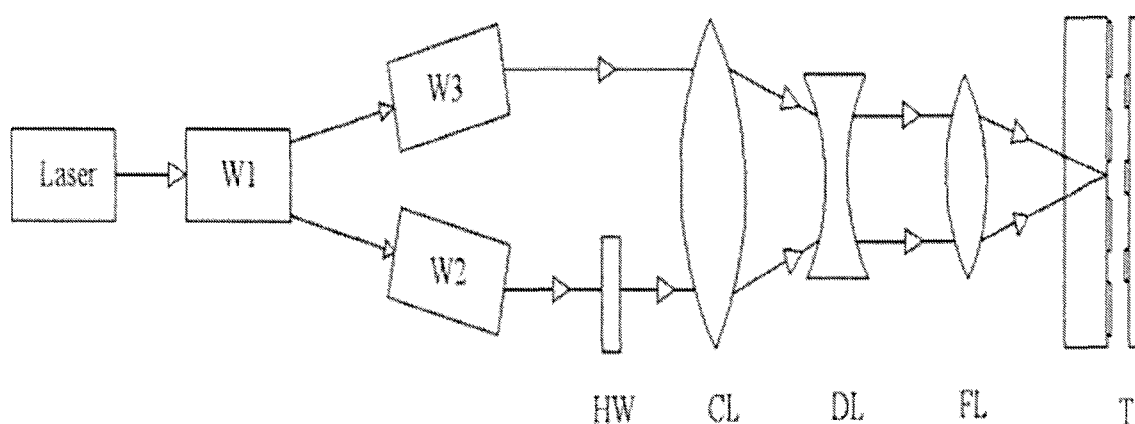
Fig 3.2 W1 – Wollaston Prism 1; W2 – Wollaston Prism 2; W3 – Wollaston Prism 3 ;

HW – Half Wave Plate; FL - Focusing Lens; CL – Converging Lens; DL – Diverging

Lens; T – Target (Donor substrate, Acceptor substrate and thin film)

This optical setup has been divided and discussed with reference to the alignment of the optical components. The first part consists of aligning of the laser beam coming from the laser system. The second major alignment is to adjust the Wollaston prisms to get parallel and equal intensity beams which are made to interfere using a focusing lens for forming patterns. This laser beam is spatially filtered and is made circularly polarized using a quarter wave plate to get orthogonally polarized light beams after it passes through the

46

first Wollaston prism. A half waveplate is placed in the path of the beam coming from Wollaston prism (W2) such that the beam impinges normal to the wave plate. For interference to happen at the focal plane the polarization of one of the beams coming from Wollaston prisms 2 and 3 has to be changed. Introduction of converging lens for alignment of the two parallel beams coming from Wollaston prisms i.e. to change the distance between the two parallel beams has been discussed further. Reduction in parallel beam spacing by a converging lens will simultaneously reduce the laser beam diameter thus varying the spot size in the focal plane. Consider a laser beam of diameter 'D' coming through the Wollaston prisms from the laser head. With the configuration shown in Fig 3.3, the converging lens would reduce the distance between two beams simultaneously reducing its diameter 'd'. This optical modification from the previous work would also change the size of focused spot at the target; thus changing pattern dimensions. The beam diameter d will also depend on the focal length 'F' of the diverging lens. Greater the focal length of diverging lens smaller will be the beam diameter 'd'.
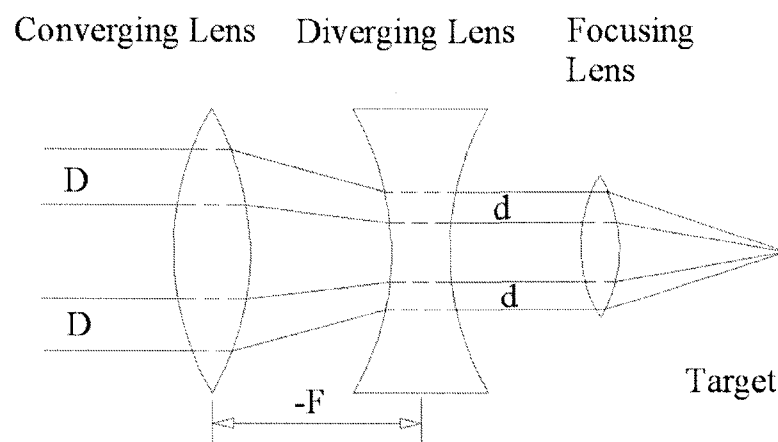
Fig 3.3 Line diagram optical setup for reduction in laser beam spacing

While setting the entire optical setup power through each of the optical element has been optimized in order to maximize output.

3.3.1 Alignment of laser

The laser system used for experiments was PRISMA NdYVO4 1064-16V. The PRISMA series provided by Coherent Inc is a solid-state Q-switch laser designed to provide optimum performance in precision industrial applications. They feature highest quality output and lower maintenance. It is a tunable system where its repetition rate can be varied from 20 to 100 KHz with an average power of 14W in the pulsed mode. The pulse width is 14 nanoseconds with peak power of 30 J/cm2 at 30 kHz [78].
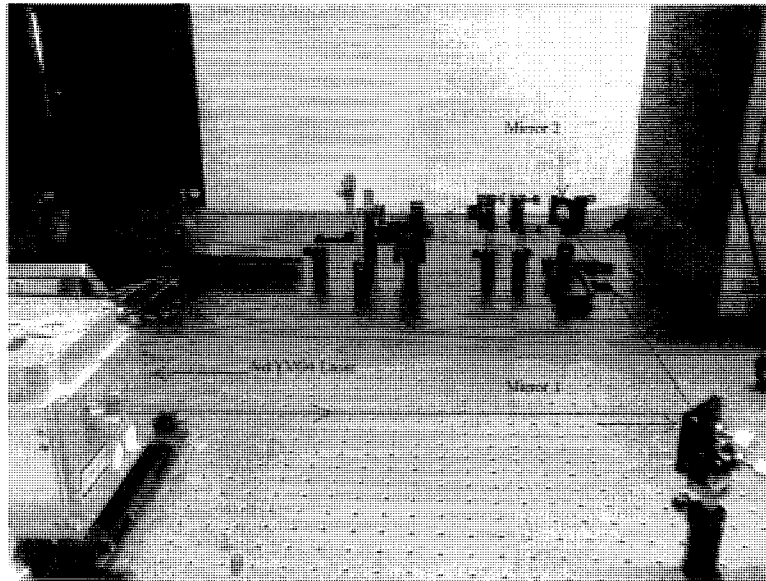
Fig 3.4 Nd:YVO₄ laser and mirrors in optical setup

Initially a laser beam of 0.8mm diameter from NdYVO4 system is expanded using a 6X beam expander to 4.8mm. Certain manipulation in beam height and orientation is

required to effectively place optical components further in this setup. Laser head being heavy makes finer adjustments difficult. Hence laser beam was made to impinge on optical mirrors 1 and 2 as shown in Fig 3.4 in order to redirect the beam coming from the laser head to a level of the optical components placed further. Infrared card was used in order to check the height of the laser beam impinging on mirrors. This initial adjustment in straightness of the laser beam is extremely important in order to avoid errors in parallelism later in the optical setup. The laser aligned for horizontal and vertical straightness was made to impinge on the first Wollaston Prism.

3.3.2 Alignment of Wollaston Prism

The optical setup consists of three 20^0 Wollaston prisms and the input wavelength of light is 1064nm. The first prism was adjusted in such a way that the laser beam coming from the laser head impinges right at its centre of aperture. Wollaston prism is an optical device that separates unpolarized light into two orthogonal, linearly polarized outgoing beams [79]. It consists of two calcite prisms cemented such that the two orthogonally polarized lights get deviated by equal measure in opposite directions. Angle of divergence is determined by the prisms wedge angle and the wavelength of the light.

A quarter wave plate is then adjusted before the first prism such that the impinging laser beam is circularly polarized and two orthogonally polarized beams coming out of it has approximately equal energy. Quarter-wave plate is used to turn linearly polarized light into circularly-polarized light and vice versa. One component of the linearly polarized light is phase shifted by $\lambda/4$ with respect to its orthogonal component to get circularly

49

polarized light. Circularly polarized light is essential requirement in order to get equal intensities in the two laser beams i.e. ($I_1=I_2$) after it comes out from the Wollaston prisms thus providing maximum visibility while interference, as discussed in predictive modeling section 2.2.1 previously. In order to get this circularly polarized light the wave plate is oriented at 45^0 to plane of polarization of the incident laser beam. The circularly polarized laser beam from the quarter wave plate is made to pass through the Wollaston prism as shown in Fig 3.5, as a result of which two orthogonally polarized beams with an angle of 20^0 between them emerges from the Wollaston prism owing to its birefringence properties.
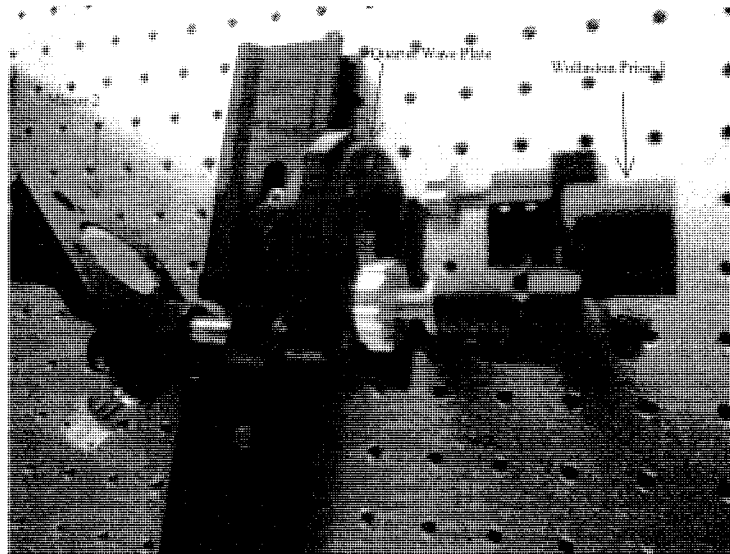
Fig 3.5 Quarter wave plate and Wollaston prisms

In order to make these orthogonally polarized beams parallel they are passed through two other 20^0 Wollaston prisms. These Wollaston prisms were mounted on the stage where

their orientation could be adjusted easily as shown in Fig 3.6. The height of the Wollaston prisms 2 and 3 shown in the figure below was adjusted such that the polarized beams from prism 1 impinge at the centre of aperture of the next two prisms. A half wave plate is aligned in the path of one of the beam axis so as to get same state of polarization in both the laser beams. Also the output beams from the Wollaston prisms 2 and 3 as shown in Fig 3.2 were made parallel along the optical axis by rotating Wollaston prisms.
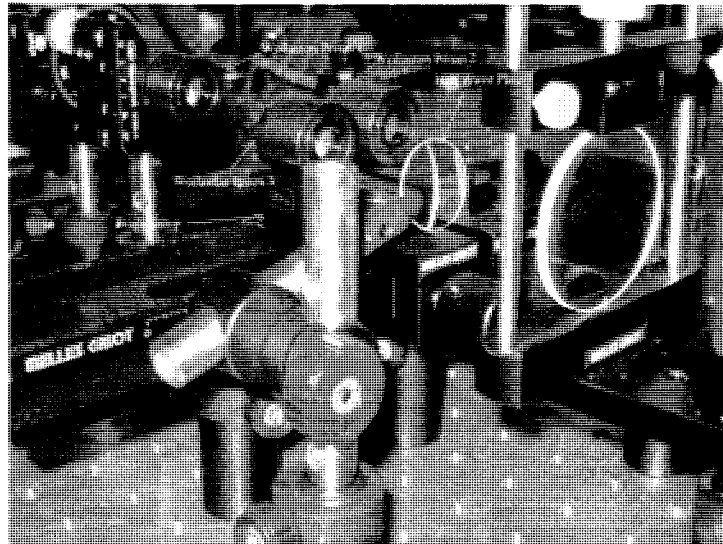
Fig 3.6 Stage of Wollaston prisms

3.3.3 Alignment of Wave plates

A wave plate is an optical device which changes polarization of a light wave passing through it. A wave plate is also called as wave retarder. It works by shifting the phase of the light wave between two perpendicular polarization components. A wave plate does not change the intensity of light; it only changes the polarization state by the principle of

birefringence. Half wave plate rotates the polarization direction of linear polarized light. It retards the polarization by half the wavelength or 180^0 [80]. This optical component is used in the setup to change the polarization of one of the beams coming from the Wollaston prisms. Hence a half waveplate was inserted in the beam path of Wollaston 2 for reversing its polarization because for interference to happen between two beams they should have same polarization. The beam coming from Wollaston prism 2 was analogous to linearly polarized light as shown in Fig 3.7. The half wave plate was mounted at an angle $\theta = 45^0$ to this beam path; thus changing the plane of polarization by $2\theta = 90^0$. The distance between the two beams with similar polarization state was measured using a ruler as 30mm.

input polarization plane

2θ

linearly polarized input

linearly polarized with plane of polarization rotated output

crystalline optic axis direction
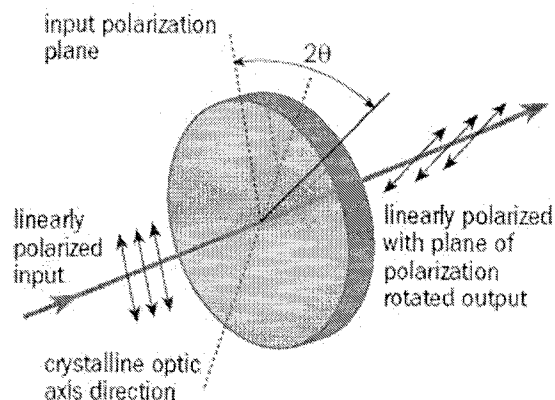
Fig 3.7 Half Wave Plate [81]

3.4   Safety Equipments

Necessary precautions while dealing with class 4 lasers are very essential. Since the $Nd:YVO_4$ is a class 4 laser and that it is out of the visible range, safety considerations

assume grater importance. It is important to make sure that at any point the beam does not deviate from its optical path. Slight change in its path can cause unknown reflections leading to hazardous effects. An infrared card and energy meter used during the experiments were potent devices to ensure safety. After each optical device alignment with respect to laser beam, beam path was checked using laser at lower power and traced by infrared card as $\lambda=1064$nm wavelength being completely invisible. Consequently after tracing its path, its power was calibrated after each optical device to calculate the power transmission efficiency in entire setup. Few types of equipment that are necessary from the safety point of view while aligning the optical setup are discussed below.

3.4.1   Optical Power Meter

LabMax-TOP is the optical power meter that consists of the sensor and a detector as shown in Fig 3.8. The sensor head could be rearranged in the optical beam path where necessary measurements had to be made.
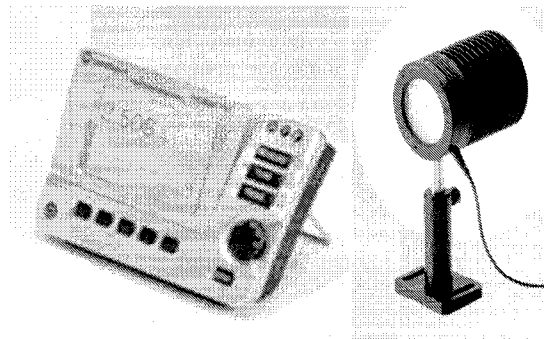
Fig 3.8 Optical Power meter [82]

The detector can be configured for the wavelength specification so as to measure its power. The damage threshold specified for the sensor was 0.6J/cm2. It is a useful device to measure the maximum energy impinging on any optical element thus preventing its damage.

3.4.2 Infrared Card

Since experiments were done in the Infrared wavelength of 1064nm, use of infrared cards and viewers thus become an important part while setting the optical setup. It helps to trace the infrared beam and thus avoid any hazards. Infrared cards as shown in Fig 3.9 were used for these experiments that could easily locate and analyze light beams in the wavelength range of 0.7–1.7 μ m. These cards are pocket sized and low-cost alternatives to an IR viewer [83]. These cards are coated with special materials which emit light when exposed to Infrared radiation.
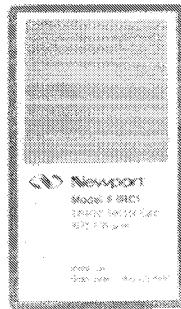
Fig 3.9 Infrared (IR) Card [83]

3.4.3 Laser Safety Glasses

Laser safety glasses as shown in Fig 3.10 are one of the most important laser safety equipment. Safety glasses are wavelength specific with particular optical density. Optical density (OD) is the absorbance of the glass for given wavelength per unit distance. Better absorbance can be obtained for glasses with higher OD. Newport laser protective eyewear's were used for these experiments. Different color of eyewear denotes its wavelength suitability.
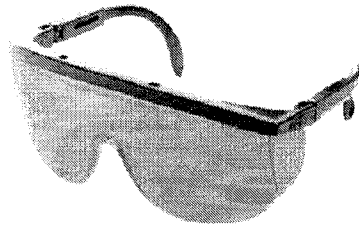
Fig 3.10 Safety Glasses [84]

3.5 Maximizing transmission efficiency

There is an optical loss associated with each of the optical device used in an optical setup. Energy meter, as shown in Fig 3.8 was used in our experiments for measuring power output from each optical element used in setup. Transmission efficiency is determined by the ratio of power output to the power input. Since Wollaston prisms affected the transmission efficiency, most its arrangement for getting maximum power has been discussed further. Only after getting maximum transmitted power from the first prism the other two prisms were arranged. The beams coming off from the first prism were at 20^0

along the axis as shown in Fig 3.11. Beam from first Wollaston prism impinged on center aperture of the following prisms.
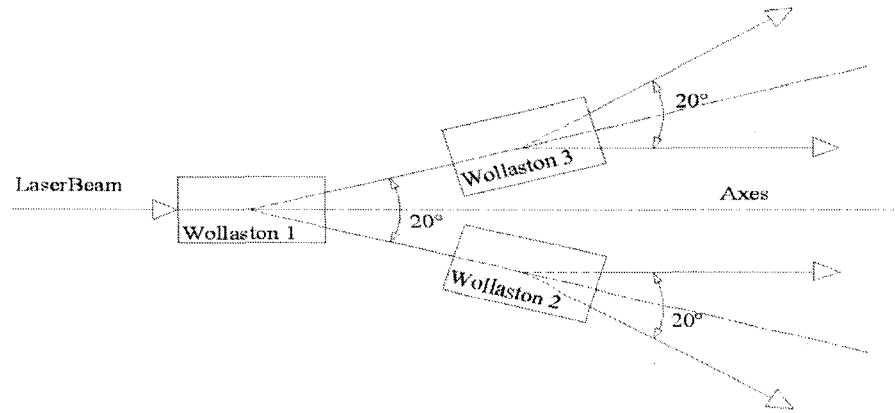
Fig 3.11 Alignment of Wollaston prisms

Since the laser beams from first prism were linearly polarized, two parallel laser beams with distance 'z' could be obtained by adjusting Wollaston prisms 2 and 3 precisely. While aligning these prisms energy loss associated with each of the Wollaston prism was observed. The loss from first prism was approximately 17.3% and other two prisms were 17.6%. These losses in the Wollaston prisms could be explained by absence of anti reflection coating. These Wollaston prisms were not designed to pass specific wavelength of light through it. Thus the maximum average transmission efficiency obtained from the Wollaston prisms was 82.55%. As per the modifications made in the optical set up; inclusion of diverging and converging lens also causes variation in transmission efficiency. Table 3.1 gives the transmission efficiency of each optical component used in the setup.

S.No.	Optical Element of Setup	Average Transmission efficiency (%)
1	Wollaston Prism	82.55
2	Converging lens (F=500mm)	92.05
3	Diverging Lens (F= -200mm)	90.35
4	Diverging Lens (F= -150mm)	91.34
5	Diverging Lens (F= -100mm)	94.15
6	Focusing lens(F=200mm)	93.82
7	Focusing lens (F=100mm)	92.8
8	Focusing lens (F=75.6mm)	90.68

Table 3.1Average Transmission efficiency of optical elements in setup

It can be seen from the table that efficiency of the focusing lens does not have much variation however it decreases with decrease in the focusing power. This may be due to more absorption by the focusing lens as its thickness increases with decrease in the focusing power. The overall transmission efficiency of the entire optical setup i.e. from laser head to focusing lens before target was calculated to be around 57%.

3.6   Obtaining parallel laser beam to get interference fringes

In order for the patterns to get deposited on the glass substrate, the interference fringes should form at the interface of the donor substrate. This requirement can only be satisfied if the two beams are parallel to each other. As shown in Fig 3.12 (B) if the two beams are

not parallel then the beams will focus before the plane of interference, thus affecting the deposition quality and requiring more energy to ablate the target material.
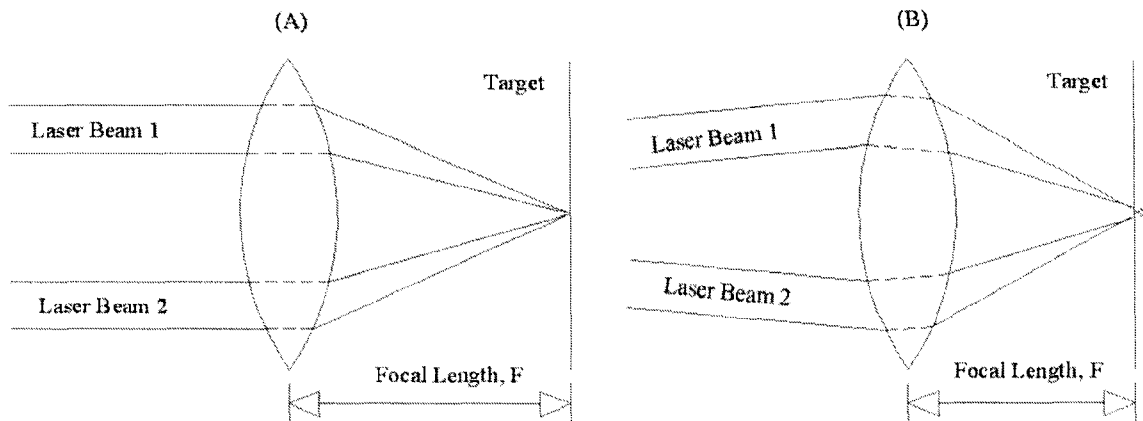
Fig 3.12 Misalignment for non parallel laser beam

In order to make these laser beams parallel, Wollaston prisms 2 and 3 shown in Fig 3.12 (B) need to be rotated finely. A mechanical rail was setup to mount a card on a stage as shown in Fig 3.13 which can freely move on the optical rail. The two laser beams coming from the two Wollaston prisms were made to impinge on this card. Two reference holes were created on the card where both the beam was made to incident at minimum power. The laser beam parallelism was approximated over the distance of the optical rail length by moving the stage on which the card was mounted. The card was moved to and fro to calibrate so that the laser beam passes through the holes made on it. At all times an IR card was held behind this card so to check passage to laser beams through the holes in the card.
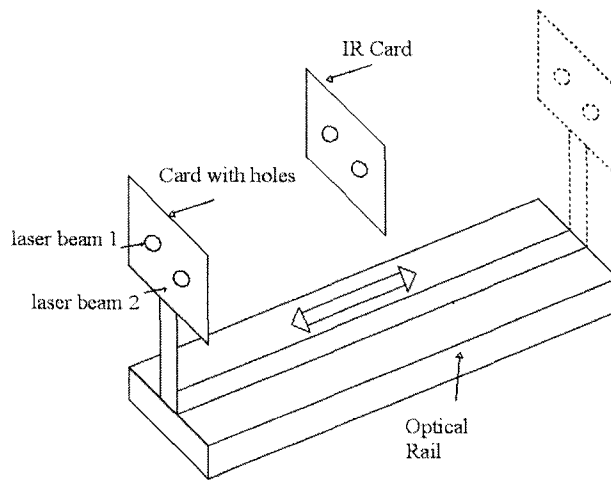
Fig 3.13 Laser beam parallelism adjustment

Once all the optics included in the setup was aligned with respect to power and position of the beam, then some optimizations were done on the setup before starting the experiments. Initially a 500mm focal length lens was used to create interference patterns at the focal plane. In order to machine the sample and set the focus accurately three steps were followed. First the LIFT target was ablated at higher energies in order to see the machining. Then the target was moved to and fro along the axis of the setup to get maximum visible intensity for its ablation. Then the laser power was tuned down to minimum possible fluence where machining was still visible, to ensure target is at the focus of the interfering beams. IR card was held behind the target al all times of this process. Since the patterns were ablated diffraction patterns were formed on the IR card shown in Fig 3.14 which tells us the patterns were ablated.
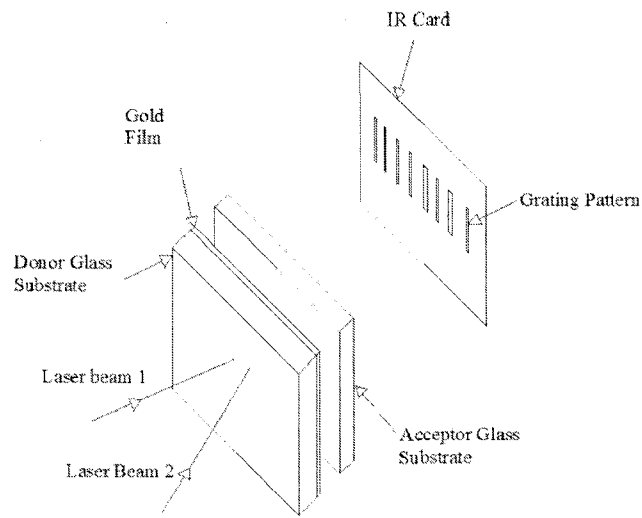
Fig 3.14 Grating Patterns on IR Card

Fringe patterns ablated from the gold donor substrate were observed in an optical microscope. Microscopic images as shown in Fig 3.15 misalignment in the patterns formed due to the interfering beams not being parallel. As seen in Fig 3.15 there are two different gold film spots not is same plane have been ablated on the glass acceptor substrate. In order to correct this error Wollaston prisms 2 and 3 were adjusted before the laser beams interfere. Rotation of the Wollaston prisms was able to remove misalignments in this patterns deposition process. Since the laser beams interfere after its individual beams are already focused as shown in Fig 3.12 (B) more power is required to ablate the gold film. It can be seen from the microscopic image Fig 3.16 that the laser beam is not able to ablate the target properly even if the beams are parallel. In other words the two beams were able to form the interference fringes but patterns ablated were not uniform. The target i.e. the donor acceptor and gold thin film were held by a mount on the stage. In order to correct in plane misalignment the first step was to adjust the

60

Wollaston prisms. Next step was to correct the orientation of the mount which holds the target. The way it is held can cause a slight tilt in its orientation of the target making it misaligned to the axis of the interfering laser beams.
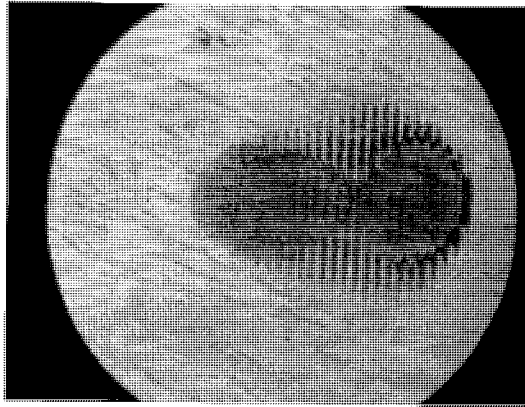
Fig 3.15 Misalignment in focused spot due to non parallel laser beams, F.O.V=100 μm
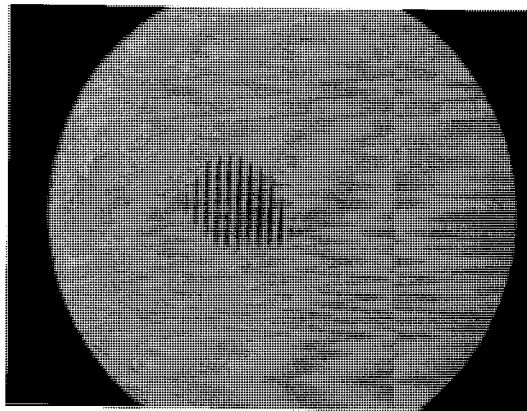
Fig 3.16 Misalignment in focused spot due to misaligned target, F.O.V= 100 μm

Different lenses with focal length i.e. 200mm, 100mm and 75.6mm were used to ablate gold fringe patterns. In order to change the distance between the two focusing beams; a negative focal length lens of 200mm mounted after 500mm focusing lens. A refined

adjustment of these lenses with respect to the two beams coming from the Wollaston prisms was necessary in order to get beams parallel as shown in Fig 3.12. The optical elements placed after the Wollaston prisms were adjusted to change the distance between the two parallel beams. In doing so the beam diameter also varies with different diverging lenses used as illustrated in Fig 3.3.

Both the beams should impinge in the central area of each of the optical element since the point at which the beams impinge on a lens greatly affect the angle at which it will focus on the focusing plane. The focusing plane in our case is the interface of the gold donor film and the glass donor substrate.

3.7   Mounting Sample on 3d axis stage

Optical stages were prepared for different experiments preformed on the target substrate. Figs 3.17 and 3.18 below show the two configurations necessary for the experiments to be preformed. In order to study the influence the laser and the setup parameters within a single spot a simple stage was setup as shown in Fig 3.17 where the target substrate could be moved along two axes i.e. in y-z direction. Movement in z direction is computer controlled using a nanomover coupled with Labview software while movement in y axis was controlled manually.
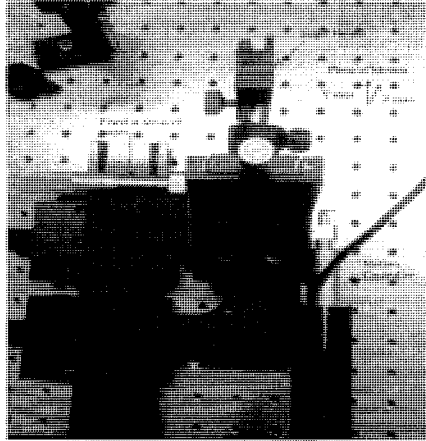
Fig 3.17 Stage for motion in two axes

However in order to scan the target sample for studying the continuity in deposition of the line patterns, a different stage having translation ability in all the 3 axis was put together on an optical rail as shown in Fig 3.18. This configuration had the ability to scan in x axis which is computer controlled while translation motion in the other two axes were controlled manually.

Fig 3.18 Stage for motion in three axes for scanning

3.8   Summary

A new optical method for depositing structured line patterns using LIFT was conceived and this simple setup was aligned for creating interference fringes at the focal point. Amplitude division was achieved with the Wollaston prisms for creating two coherent light beams. Advantages associated with this setup were that the common optics could be used with this setup as the spacing between the two parallel beams can be easily varied just by changing the diverging lens. Transmission efficiency of the setup was more than 50% with all the optics used and the alignment and safety of the setup has also been discussed. Misalignments in the setup can be easily adjusted for good quality ablation of thin film from DS. Further experiments were done using this optical setup as discussed in next section.

CHAPTER 4   EXPERIMENTAL RESULTS AND DISCUSSION

4.1   Introduction

Experiments were done by configuring the setup discussed in the previous chapter. Sample was clamped on the holder that was arranged on the optical rail in order to have a 2 axis movement as shown in Fig 3.17. All the experiments were performed in ambient conditions. Experiments were done initially by maintaining the distance between acceptor substrate and donor film at $60\,\mu m$. However no depositions were observed other than close contact mode owing to higher reflectivity and lesser absorption of gold film in infrared region (i.e. 1064nm); therefore all the experiments were performed in contact mode as shown in Fig 3.1. Experiments were done in two parts; first part of experiments were done to optimize laser parameters (e.g. energy, repetition rate), whereas in the second set of experiments the optical setup was optimized for quantity and quality of deposition. AFM images and optical micrographs were used to evaluate and to understand optimum laser and setup parameters for the deposition of good quality gold line patterns and for comparison with predictive modeling.

4.2   Influence of energy on deposited pattern

Experiments were done at different energies to deposit the gold fringe patterns on the glass substrate. Patterns deposited on the substrate were ablated from the acceptor gold substrate coated with gold film 50nm in thickness. Gold line patterns were deposited at three different energy levels low $(0.5\text{-}1.3)\text{J/cm}^2$, medium $(1.3\text{-}3.5)\ \text{J/cm}^2$ and high $(3.5\text{-}5)$

J/cm^2 as shown in Fig 4.1(a-p) and 4.2(a-p) in order to study the effect of laser energy on deposition of these patterns.

(a) 0.53J/cm^2	(b) 0.65J/cm^2	(c) 0.75J/cm^2	(d) 0.85J/cm^2	(e) 1.27 J/cm^2
(f) 1.44J/cm^2	(g) 2.03J/cm^2	(h) 2.25J/cm^2	(i) 2.90J/cm^2	(j) 3.17J/cm^2
(k) 3.70J/cm^2	(l) 4.00J/cm^2	(m) 4.40J/cm^2	(n) 4.60J/cm^2	(o) 4.98J/cm^2
(p) 5.02J/cm^2				
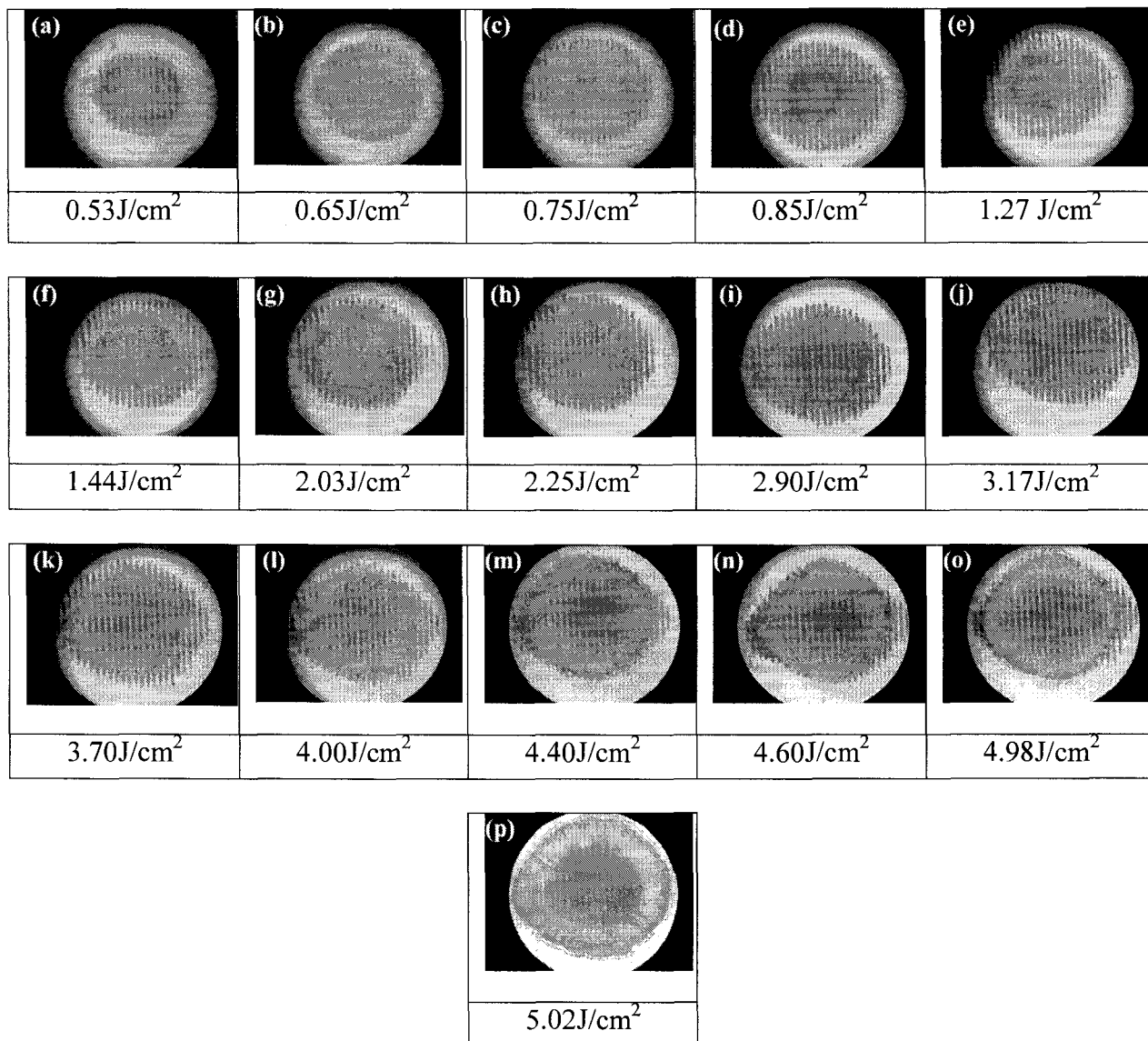
Fig 4.1 (a-e) Ablated gold film fringe patterns between (0.5-1.3)J/cm2 low energy, (f-j) Ablated gold film fringe patterns between (1.3-3.5) J/cm2 medium energy, (l-p) Ablated old film fringe patterns between (3.5-5) J/cm2high energy, time =1 sec, 20kHz repetition rate, focal length=75.6mm. F.O.V=100 μm
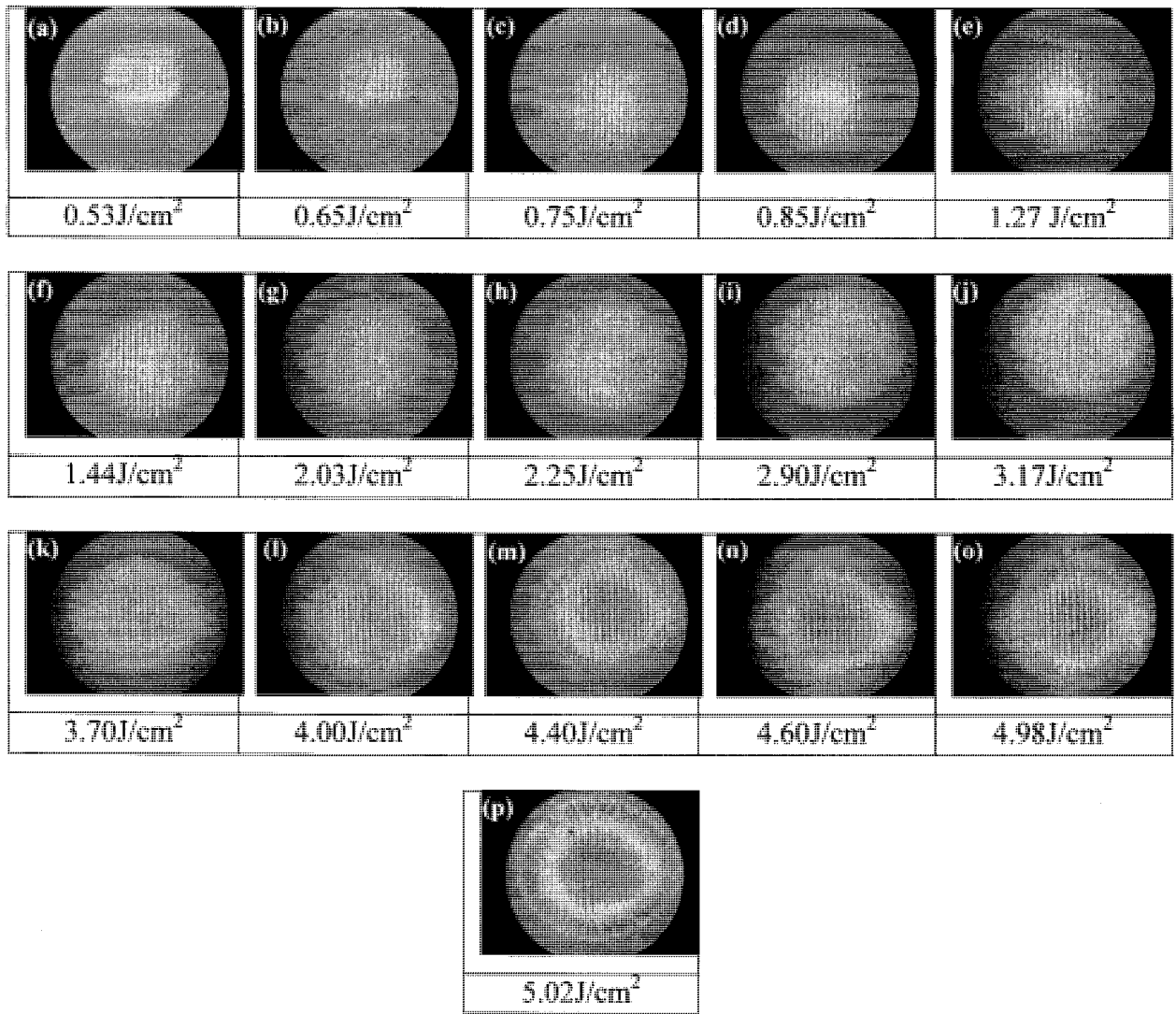
Fig 4.2 (a-e) Deposited gold film fringe patterns between (0.5-1.3)J/cm2 low energy, (f-j) Deposited gold film fringe patterns between (1.3-3.5) J/cm2 medium energy, (l-p) Deposited gold film fringe patterns between (3.5-5) J/cm2high energy, time =1 sec, 20kHz repetition rate, focal length=75.6mm. F.O.V= 100 μm

From the Fig.4.1 and Fig 4.2 it can be concluded that with the increase in laser power there is an increase in the ablated spot size. Fig 4.3 shows a graphical comparison of the variation in the ablated and the deposited spot size with respect to laser energy. Also the

theoretical prediction of the ablated spot size from section 2.3 is plotted in the figure for comparison.
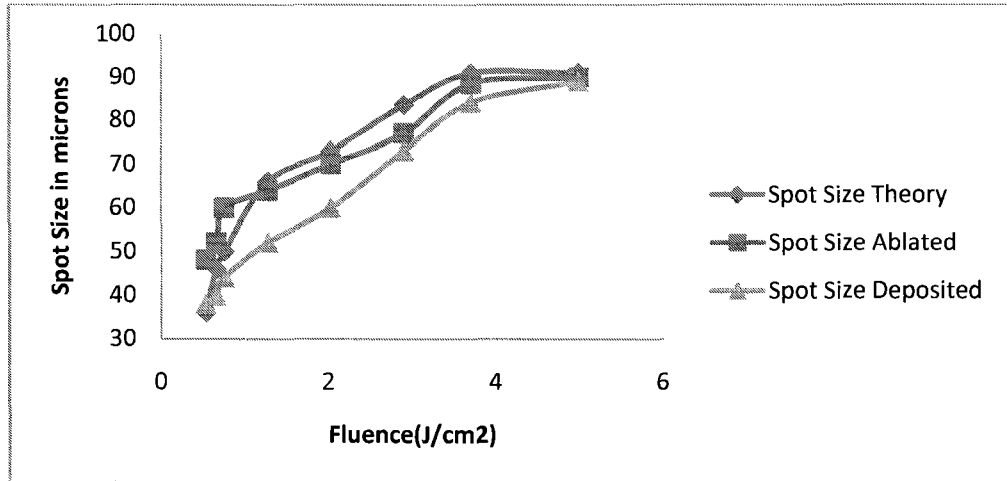
Fig 4.3 Graphical comparison of spot size variation with fluence energy

As shown in Fig 4.3, a comparison has been made with the ablated spot size and spot size obtained by theory. As the energy of the laser beam increases, larger area within the Gaussian curve will have energy higher than the threshold of Chromium, to soften it thereby ablating more fringes from the DS. The difference in the spot size at lower fluences in the figure above can be attributed to thermal nature of ablation with nanosecond lasers in which threshold fluence is not clearly defined. Even though the ablation threshold of chromium is $1.5J/cm^2$, fringes were ablated for lower fluence of $0.53J/cm^2$ as the peak power is able to soften chromium but not able to ablate it as discussed in section 1.5.4. However at higher fluence the variation is minimal in spot size due to possible absorption by the DS. A comparison has also been made in ablated and deposited spot size which can give exact efficiency of line pattern deposition, called as

percentage deposition. Percentage Deposition is the ratio of the number deposited line patterns to ablated line patterns. Here the number of line patterns will increase and so will the dimension of the deposited spot. The gold fringe patterns were observed to get deposited at lower energy of $0.53 J/cm^2$ as seen in Fig.4.2 (a). It can be seen in Fig.4.2 that with increase in the energy to $1.44 J/cm^2$, the deposits of patterns is significantly increased. The deposition of the gold fringe patterns are well defined while the laser energy is in between $0.75 J/cm^2$- $1.44 J/cm^2$ as seen in Fig4.2(c, d, e, and f). Also the number of fringes deposited with respect to ablated fringes increases with increase in fluence.

Sr. No.	Fluence (J/cm2)	%Deposition
1.	0.53	33
2.	0.65	38
3.	0.75	60
5.	1.44	77
6.	3.17	87
7.	4.00	96
8.	4.98	96.2

Table 4.1 Comparing efficiency of deposition with fluence

It can be seen form Fig 4.1(e-p) and 4.2(e-p) that that at intermediate and higher energies; maximum coverage can be obtained for ablated and corresponding deposited patterns. Summary of the coverage in terms of percentage deposition is shown in the table 4.1.
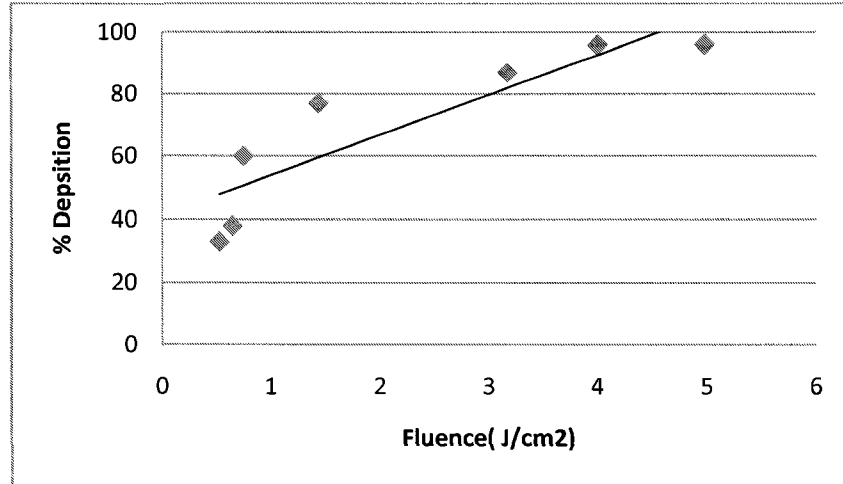
Fig 4.4 Graphical comparison of efficiency of deposition with fluence

It can be seen from Fig 4.4 that efficiency of deposition increases with increase in energy. In the deposition range where the efficiency is 60% to 84%, good quality fringe patterns can be maintained but at higher energies the central deposited fringes starts thinning. Though greater deposition efficiency can be achieved at energies above 4J/cm2; the quality starts diminishing and the deposited gold film spreads outside of the focused spot area. View of the micrographs of fringe pattern deposited at high energies, shown in Figs 4.5 and 4.6 would enable us to better understand the quality of the deposition. It can be seen clearly in Fig 4.5 that at higher energies gold material deposited in one fringe starts accumulating on the edges of a fringe pattern. The dark area on the edges of each fringe shows that excess heat is involved in deposition of the patterns.
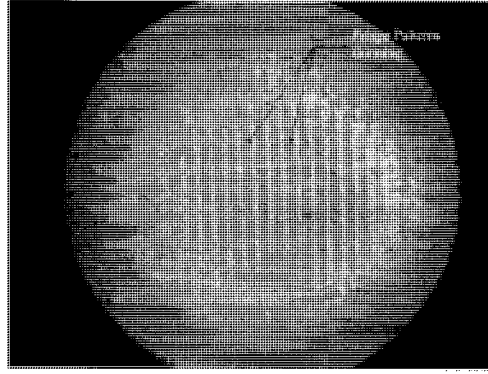
Fig 4.5 Gold fringe pattern thinning at energy at 4.00 J/cm2 energy, time =1 sec, 20 kHz

repetition rate, focal length=75.6mm. F.O.V=100 μm

This process of thinning becomes more visible for pulse powers greater than 4J/cm2 where the patterns starts disappearing and the gold material starts depositing on the periphery of the patterned spot shown in Fig.4.6.
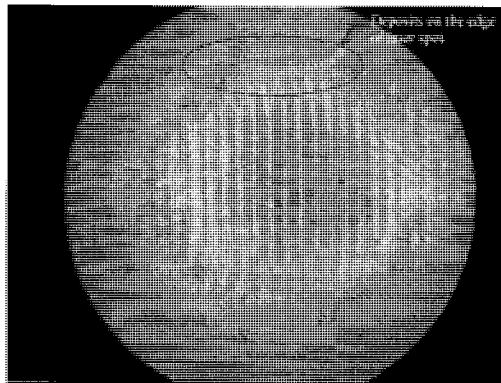
Fig 4.6 Gold material deposition on the periphery of the deposited pattern at 4 J/cm2

energy, time =1 sec, 20 kHz repetition rate, focal length=75.6mm. F.O.V= 100 μm

Fig.4.6 can be explained by phase explosion phenomenon in the deposition process of the fringe patterns. At higher pulse energies the deposited gold film spreads outside of the

focused spot area, possibly because of transition to boiling phase. Miotello and Kelly (1995) explained that phase explosion is an explosive liquid-vapour phase change, due to homogeneous nucleation of vapor in a superheated liquid [85].

4.3 Machining with different repetition rates

Experiments were performed to study the effect of repetition rate on the fringe pattern formation. Repetition rate defines the number of pulses hitting the target per second. Since the average power is constant, variation in repetition rate varies the peak power (as shown in Fig 1.7) and thus the fluence to ablate the thin film for line pattern deposition.
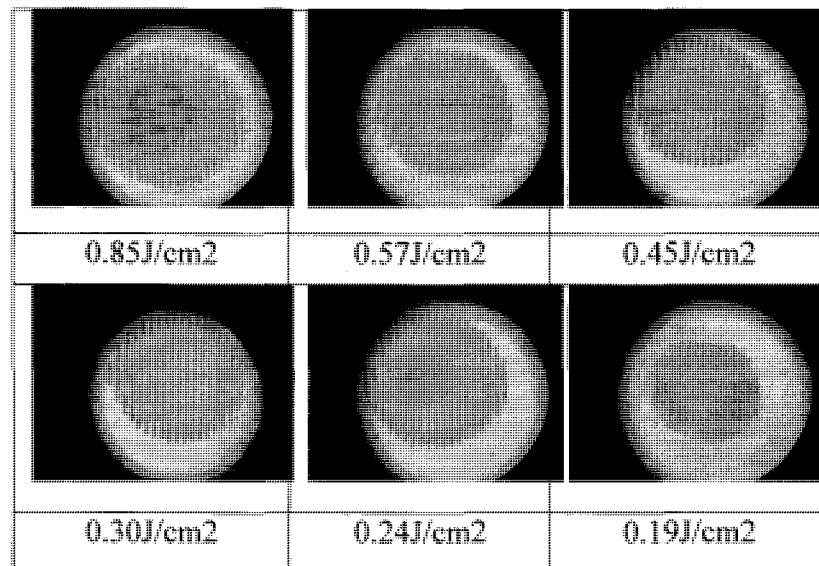
Fig 4.7 Patterns ablated from donor substrate at focal length lens=75.6mm (a) 20 kHz (b) 30 kHz (c) 40 kHz (d) 60 kHz (e) 80 kHz (f) 100 kHz. F.O.V= 100 μm

72

0.85J/cm2	0.57J/cm2	0.45J/cm2
0.30J/cm2	0.24J/cm2	0.19J/cm2
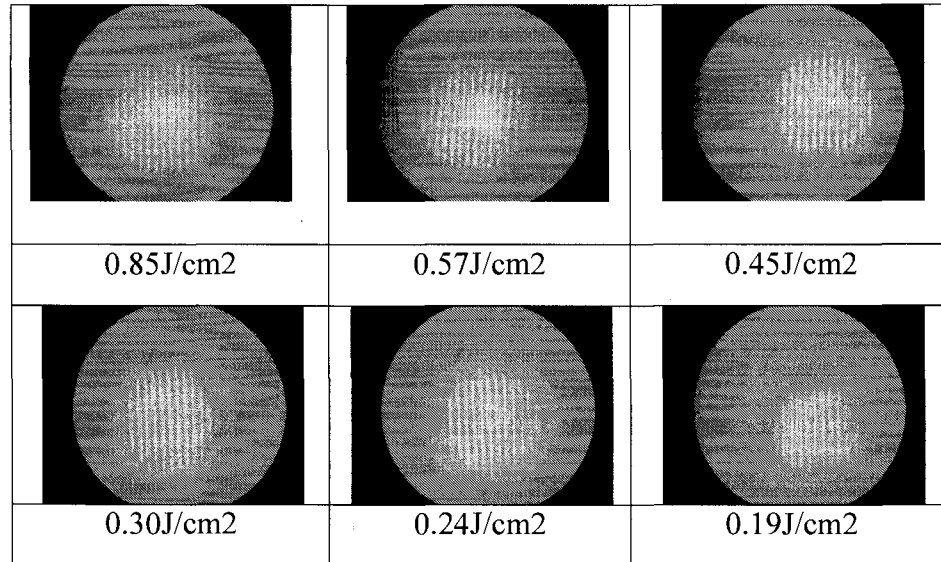
Fig 4.8 Corresponding Fringe pattern deposition for ablation shown in Fig4.8

It can be concluded from Fig.4.7 and Fig 4.8 that with increase in the repetition rate the spot size of the ablated and deposited patterns decreases. Maximum coverage of the fringes can be observed at a repetition rate of 20 kHz; however with increase in the repetition rate above 40 kHz the number of fringe patterns starts decreasing, this effect is attributed to decrease in energy with respect to increase in repetition rate. Energy of a pulse is defined as the ratio of average power to repetition rate. This explains that more number of pulses would be hitting the target in 1 second, thus increasing the average power marginally while reducing its peak power significantly. Comparison has been made in the ablated and the deposited fringes in order to study the efficiency of coverage as shown in table 4.2 in terms of percentage deposition by variation in repetition rate as explained earlier.

Sr. No.	Energy (J/cm2)	%Deposition
1.	0.85	61.9
2.	0.57	61.9
3.	0.45	55
4.	0.30	54.3
5.	0.24	50
6.	0.19	50

Table 4.2 Comparing efficiency of deposition by varying repetition rate
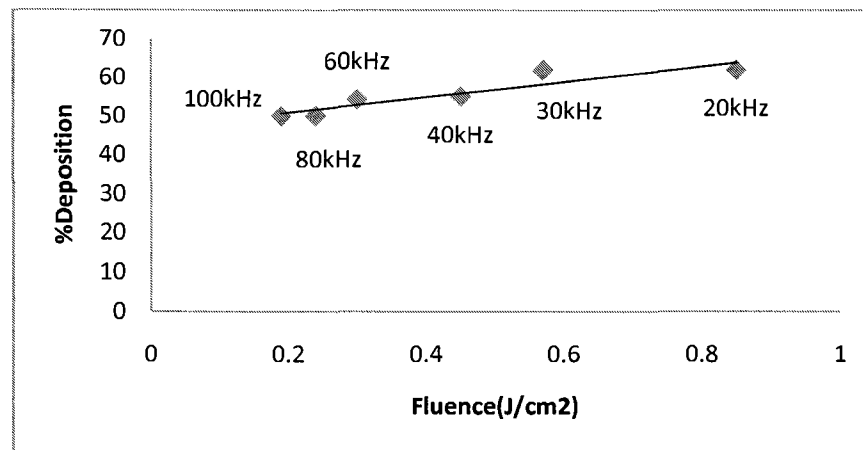
Fig 4.9 Graphical comparison of efficiency of deposition with energy

Fig 4.9 clearly indicates better efficiency of deposition at lower repetition rate where the laser energy is higher compared to higher repetition rates. X axis represents the peak power available at the respective repetition rates used in the experiments.

4.4   Influence of optical setup parameters on deposited patterns

Variation in the interference patterns can be created by changing the angle between the two beams at the focal plane. We can change the angle by changing the diverging lens that will change the distance between the two parallel beams or by using different focusing lenses. The Fig 4.10 illustrates the possible variations in the optical setup to modify the patterns deposited on the glass substrate. From the equations 4.1 and 4.2 the angle between the two beams θ is the function of Z and F. However this angle would vary and be limited to focal length. The glass donor substrate would limit the bend of the laser beams thus causing variation in pitch of the fringe patterns ablated and deposited as discussed in section 2.5 of the theoretical modeling.

Laser Beam 1

Distance Between
Parallel Beams   Z

θ

Laser Beam 2

F
Focusing Length
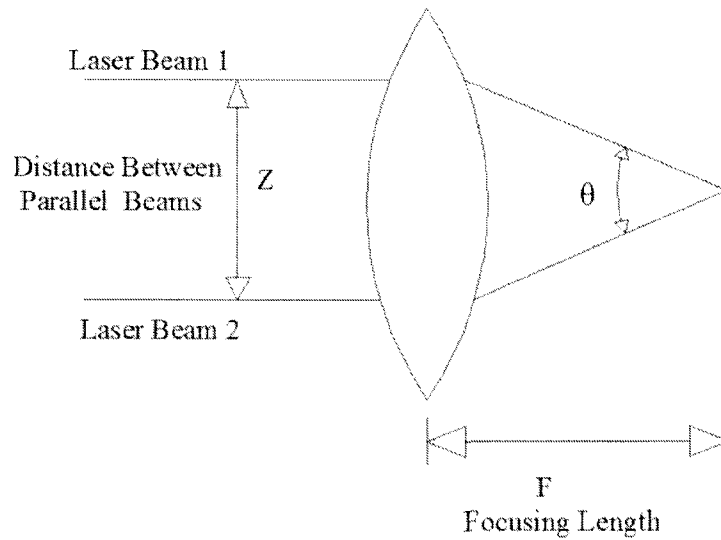
Fig 4.10 Variation in distance to vary pitch of the patterns deposited

$$Pitch = \lambda/2Sin\ (\theta/2) \qquad\qquad (4.1)$$

$$\theta/2 = tan^{-1}(Z/2F) \qquad\qquad (4.2)$$

75

4.5   Gold Pattern deposition by varying focusing lens

Experiments were done at different focusing lenses in order to vary the pitch of the fringe patterns deposited on the acceptor substrate. According to the proposed optical setup the pitch of the deposited line patterns by either changing the focusing lens or by varying the distance between the two beams that interfere. The variations caused are compared with the ablated features on the gold donor substrate, simultaneously its effect on the deposited patterns are also discussed.

For this experiment three lenses with focal lengths 200, 100 and 75.6 mm were used. Throughout this experiment the beam spacing was maintained at 13mm. The variation in the fringe spacing has been shown with the help of optical micrographs of ablated and the deposited gold feature patterns in Fig 4.11.

It can be seen from the optical micrographs that the pitch of the ablated patterns was smallest for the focusing lens of 75.6mm. When the F is increased to 100mm and 200mm the pitch of the ablated patterns increases. Very fine deposited patterns were observed with lower focusing lens of 75.6mm. It can be seen in Fig 4.11(a) that spacing between the fringe patterns deposited with focusing lens of 75.6 mm were of good quality and clean on the edges. It was observed that that the gold fringe patterns were deposited at a lower energy by focusing lens of 75.6mm in comparison to other two lenses since with this smaller spot size could be obtained enabling more energy available per unit area for ablation of fringe patterns.
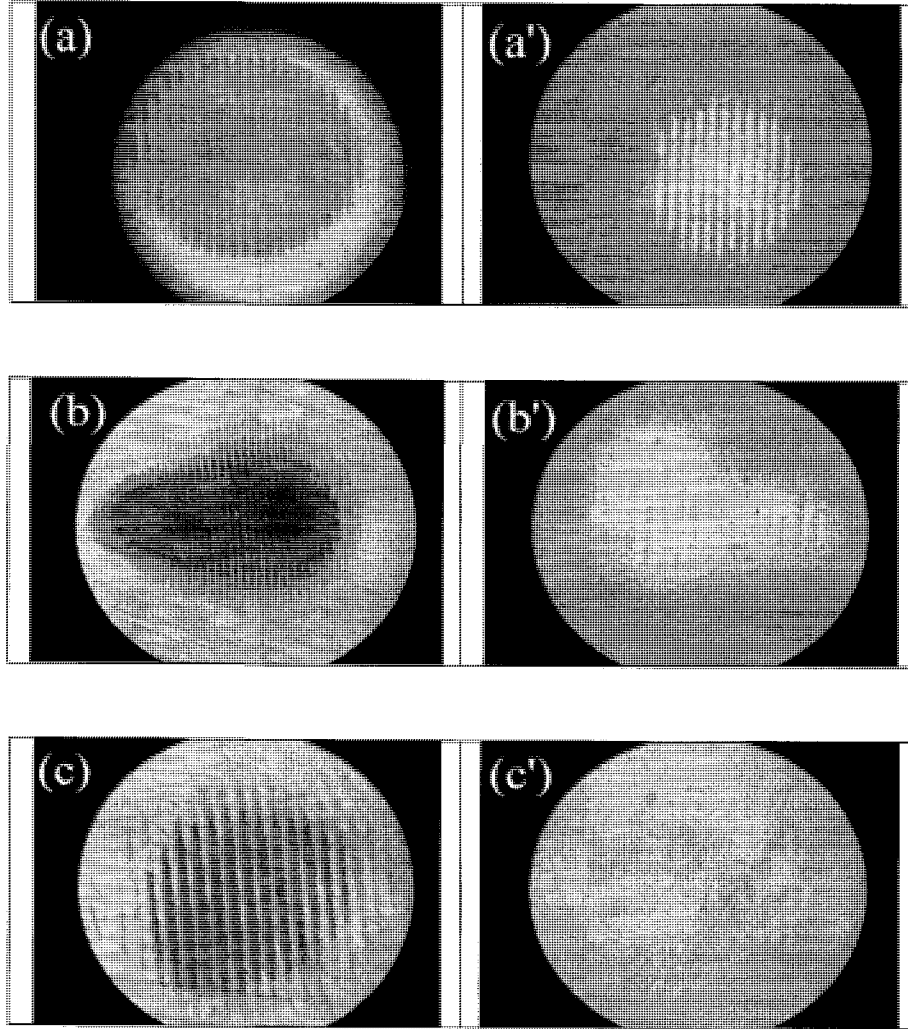
Fig 4.11 Gold fringe patterns ablated and deposited, repetition rate of 20Khz, distance

between the beams z=13mm (a,a') Focusing lens F=75.6mm (b,b') Focusing lens

F=100mm (c,c') Focusing lens F=200mm. Fluence energy 2.9J/cm²

Negligible and poor quality depositions were observed for the other two focusing lens for

the same energy. The reason for this is that by using a lower focusing lens more energy of

the laser beam is concentrated in very small area of a spot. Hence well defined and better

quality deposition is observed at lower focal lengths. Table 4.3 shows the comparison of

experimental and theoretical values of the pitch computed using equations 4.1 and 4.2 ablated from the donor substrate.

Sr.No	Focal Length (mm)	Theory (μm)	Experiments (μm)	Error %
1	200	16.4	20.5	20
2	100	8.2	10	18
3	75.6	6.8	8	15

Table 4.3 Pitch values at different focusing lens

It can be seen from Table 4.3 that % error is high predominantly due to the fact that the thickness of the donor substrate and its refractive index plays a significant role in the angle of the focused beam and the achievable focus spot size as discussed in section 2.5 and as shown in Fig 2.6. Table 4.4 and Fig4.12 show the experimental and the theoretical data while considering the effect of the donor substrate. It can be seen from table 4.4 that the error % reduces a lot and difference between experimental and theoretical values is less than 0.9 μm.

Sr.No	Focal length (mm)	Theory (μm)	Experiments (μm)	Error %
1	200	19.6	20.5	4.3
2	100	9.3	10	7
3	75.6	7.4	8	7.5

Table 4.4 Pitch values at different focusing lens considering the effect of DS

This can be attributed to measurement errors were a ruler was used determine the distance between the laser beams. A graphical comparison in order to study the variation in pitch with focal length of lens has been made. From Fig 4.12 it can be concluded pitch obtained experimentally is more than theoretically due to plume explosive phenomenon in outward direction. It can also be concluded that minimum possible pitch of 8 μm could be obtained with 75.6mm lens. Depending on the requirement this could be reduced further by either using a smaller focal length lens or by increasing the distance between the interfering beams. With increase in the focusing length, pitch of the ablated patterns can be increased while simultaneously increasing the pitch of the deposited feature patterns.
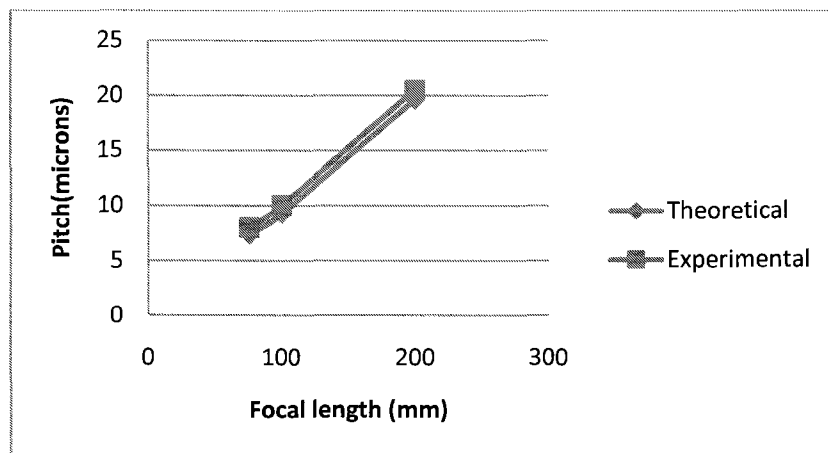
Fig 4.12 Graphical Comparison of Experimental and Theoretical results

Variation in the ablated patterns will also cause variation in the deposited pattern features. Since no deposition was observed for lower energy with focusing lens of 200 and 100mm percentage deposition is compared only at higher energies for each focal

length lens as shown in Fig 4.13. This comparison is done with deposition of patterns before thinning of fringes occur as discussed earlier in section 4.2 (Fig 4.5).
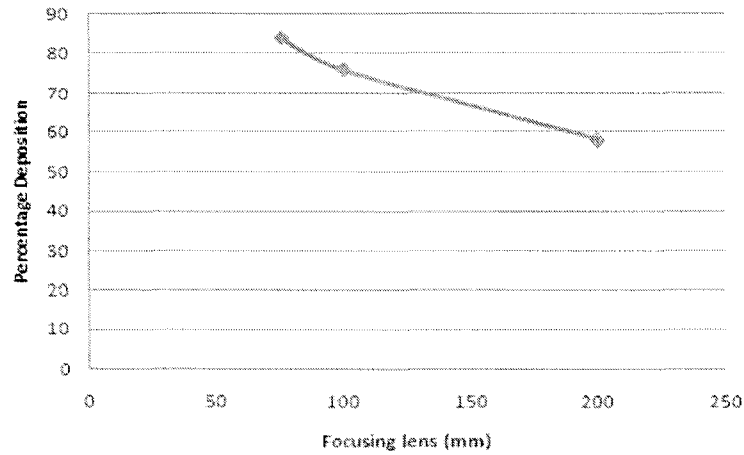
Fig 4.13 Comparison of percentage deposition at varied focal length

It can be seen from the Fig 4.13 that lower focusing lens has highest coverage in terms of ablated to the deposited gold patterns. Also for a particular focusing lens the distance between beams can be varied for fringe pattern as shown in next experiment.

4.6   Pitch variation by varying distance between two laser beams

Gold film was ablated from the donor substrate using a lens of 100mm focal length. This experiment was done with varied beam spacing's of 7mm, 9mm and 13mm using diverging lens of 100,150 and 200 respectively. These beam spacing's were obtained with different set of diverging lenses. Distance between the two beams was measured manually. Fringe patterns ablated and deposited with each of the beam spacing created a different pitch while deposition. The thickness of the gold film was maintained at 50nm

for this experiment. These fringe patterns are verified with the help of optical micrographs as shown in Fig 4.14.
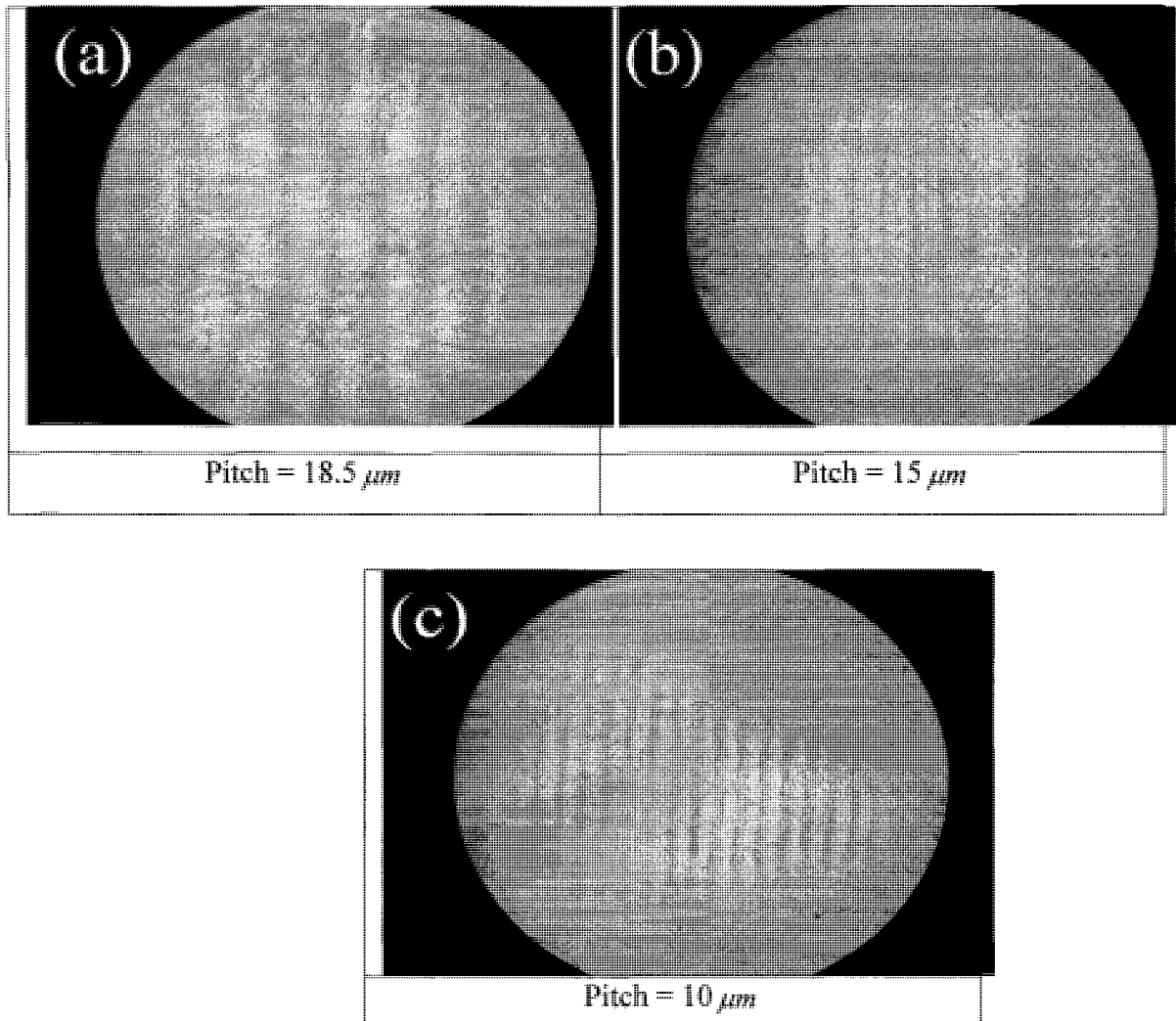
Fig 4.14 (a) Fringe patterns deposited at a beam spacing of Z=7mm, rep.rate of 20Khz, time of 1seconds and energy of 3.7 J/cm² (b) Fringe patterns deposited at a beam spacing of Z=9mm, rep.rate of 20Khz, machining time of 1seconds and energy of 3.7 J/cm² (c) Fringe patterns machined at a beam spacing of Z=13mm, rep.rate of 20Khz, machining time of 1seconds and energy of 3.7J/cm²

Experiments were compared with the theoretical pitch value obtained from the equations

(4.1) and (4.2).

Sr.No	Beam Spacing (mm)	Theory (μm)	Experiments (μm)	Error %
1	13	9.3	10	7
2	9	14.8	15	1.3
3	7	18.2	18.5	1.6

Table 4.5 Comparison of experimental pitch with theoretical pitch
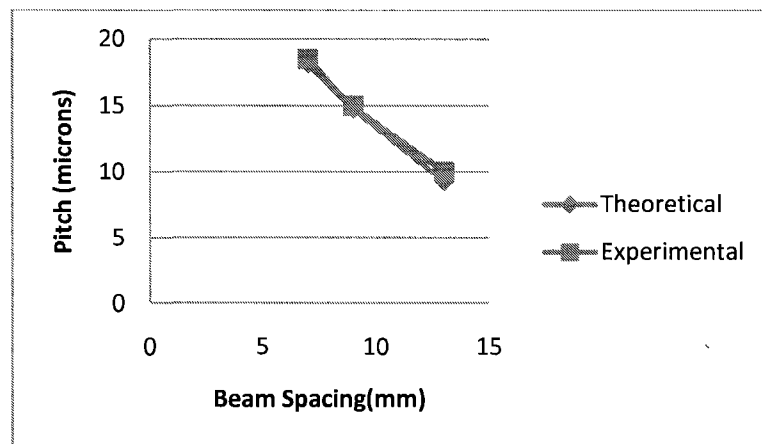
Fig 4.15 Comparison of theoretical and experimental pitch values

It can be interpreted from the Table 4.5 that the pitch obtained experimentally is more than theory due to plume motion in outward direction as discussed in the section 4.5. As a result there will be a spread in the fringe patterns deposited. Fig 4.15 shows that the variation in pitch with respect to beam spacing was according to the given theory. It can be concluded from the graph that as the distance between the two parallel beams increases the pitch of the fringe patterns deposited decrease and vice versa

4.7   Effect of donor film thickness on deposition of fringe patterns

Donor glass substrate was coated with different thickness of gold film. Experiments were performed using gold thickness of 50nm, 100nm and 200nm on the donor substrate. Patterns were deposited at a constant pulse energy using a 100mm focusing lens. Fig 4.16 shows deposition of patterns at different thicknesses. It can be seen from the Fig 4.16 that as the thickness of the gold film increases on the donor substrate lesser number of fringes are deposited on the acceptor substrate. As the film thickness reaches 200nm more energy is required to ablate and deposit the gold film. As gold film being highly reflective in nature lesser deposition is observed at higher thicknesses. This variation can be explained by the theory that there are two kinds of forces involved in the film removal process, one being the vapor force and the other is the shearing force. Since the distance between the donor and the acceptor is kept minimal external force does not have much of impact on film removal process. Hence the shearing force required to ablate and deposit the fringe patterns becomes a direct function of the film thickness.

The trend of the variation in the force and energy required to ablate a particular thickness of film has been shown with the help of plot shown in Fig 4.17. There cannot be a direct comparison of the values for this variation but the trend of variation remains the same as explained in the theoretical modeling. It can be seen from the plot that the force required to deposit the gold film with film thickness increases. This trend can also be seen in terms of energy where energy required to ablate the film also increases with film thickness and vice versa.
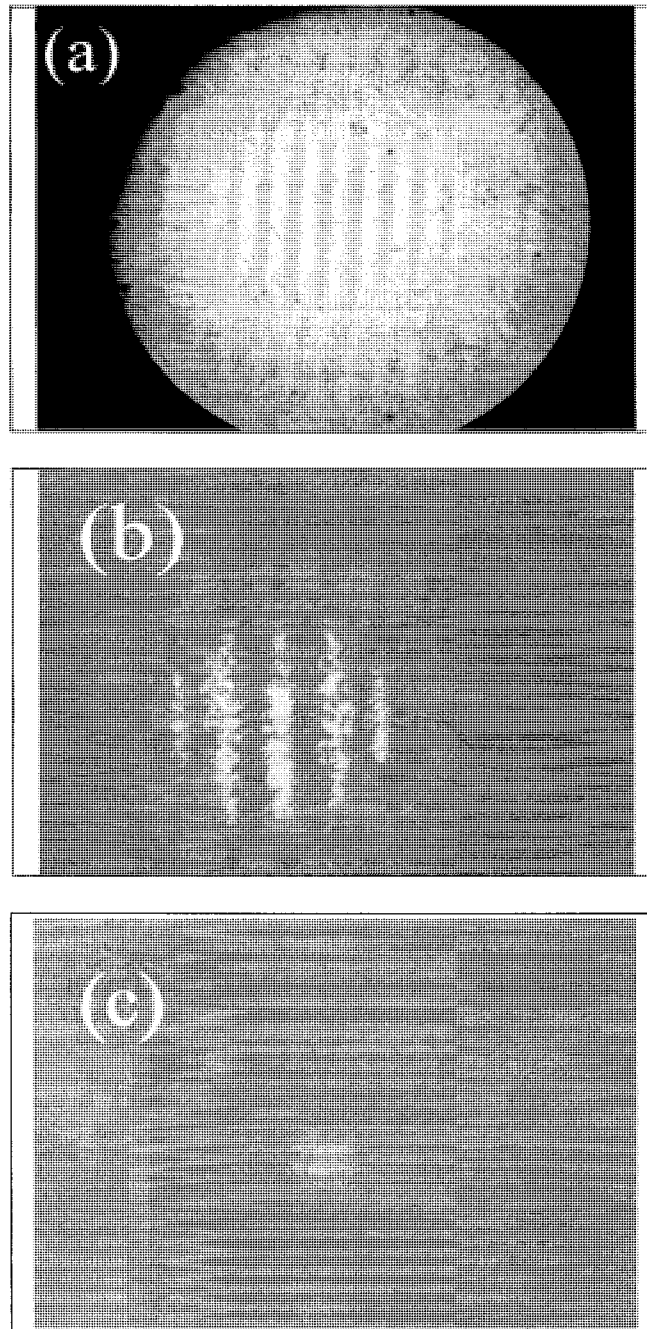
Fig 4.16 Gold Fringe Patterns deposition at different thicknesses, Focusing lens=100mm, Repetition rate =20 kHz (a) 50nm (b) 100nm(c) 200nm. Fluence=4J/cm²
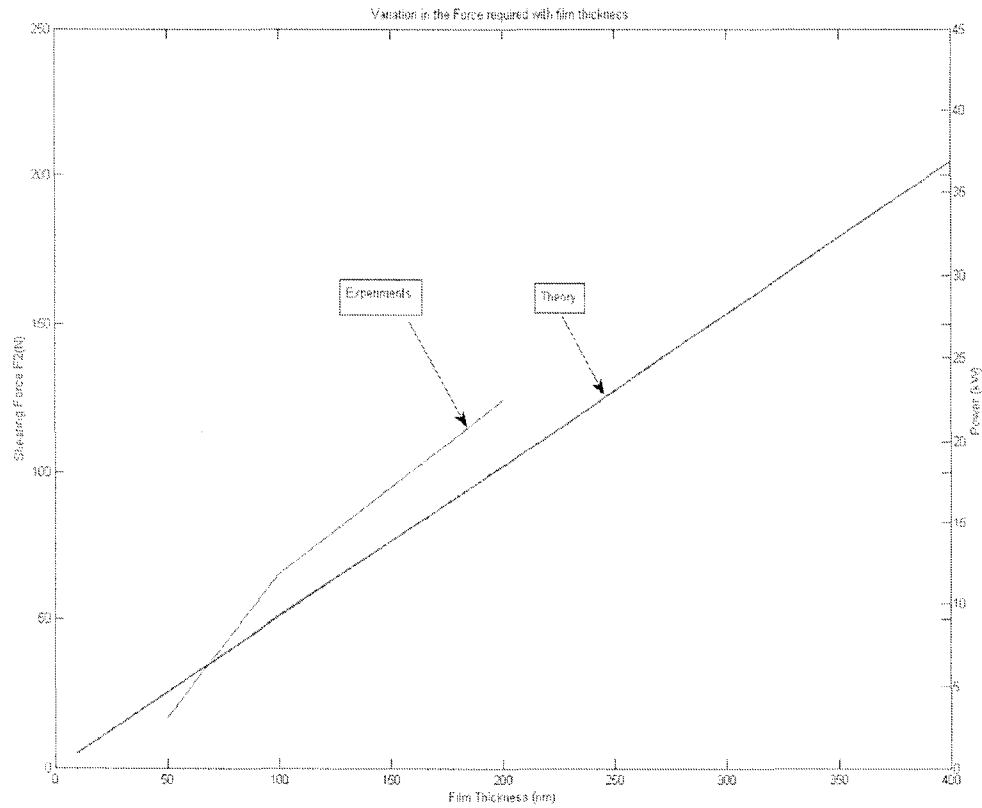
Fig 4.17 Theoretical and experimental comparison of force required for ablation of gold film with film thickness

4.8 Continuity of Fringe Patterns

In order to make the proposed technique viable for patterning applications, continuity experiments for pattern deposition were done. Experiments were done with 500mm focusing lens where the distance between the two beams was kept to 30mm. The thickness of the gold sample was maintained at 50nm. A stage as shown in Fig 3.16 was setup in order to mount the sample as scanning was required on the surface of the sample. Different feed rates and dwell times were considered to study their effect on continuity of deposition. While continuous ablation was possible with almost any variation of the feed

rates and dwell times, continuous deposition was possible only at few ranges. In the experiments done before, it took 1 sec for to gold film to ablate and deposit on the AS. In order to maintain continuity similar dwell time of 1 sec was programmed after a given feed rate while scanning. Dwell time is the time the motion controller is programmed to stop after which it again starts the motion with constant velocity feed rate. Fig 4.18 shows the trend of feed rate and dwell time that was programmed using labview software.
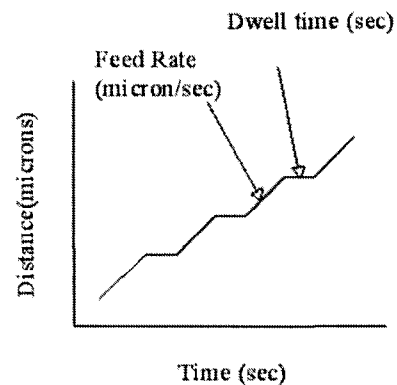
Fig 4.18 Trend of dwell time and feed rate

The feed rate was selected in such a way that controller traverses the distance that covers 25%, 40% and 75% of the original spot size of $270\,\mu m$. Fig 4.19 shows the direction of scan and the spot overlap condition at its respective feed rate. Attempts were made for getting the continuity of the gold fringe lines by manipulating spot overlaps. Although ablation was observed over the length on the donor substrate there was no deposition seen on the glass substrate. The reason may be that an appropriate orientation of the sample is required while scanning the sample over a length. A slight tilt in the target substrate may

be one of the reasons for no deposition. Fig 4.20 shows one such attempt where the ablation happened with no deposition on the glass substrate.

Scan
Direction

25% overlap   40% overlap   25% overlap
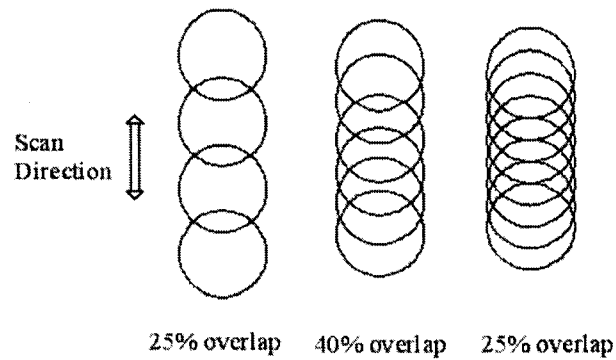
Fig 4.19 Spot overlap conditions for scanning the patterns

However at a certain instance as shown in Fig 4.21 the deposition observed was continuous over a length 3 times more than the actual spotsize. The Fig below shows a scanning length over 700 μm with velocity of 160 μm /second for line pattern deposition. Result was obtained for approximately 40 % spot size coverage.
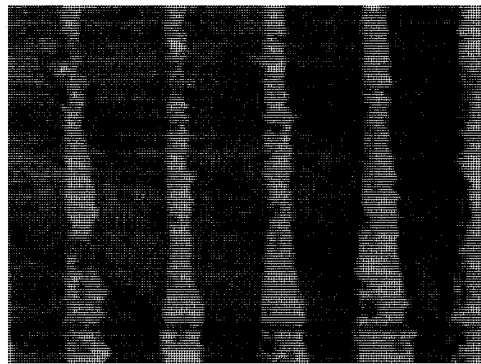
Fig 4.20 Gold fringe lines ablated on the donor substrate with 25% overlap in focused

spot. F.O.V= 50 μm

Fig 4.21 Gold fringe pattern scanning at velocity 160 µm /second

4.9   Quality of deposition: AFM analysis

Pulse energy has significant effect on the quality of the fringe pattern deposition. The quality of the patterns deposited has been discussed with the help of Atomic Force Microscopy results as shown in Fig 4.22. Patterns deposited were homogenous and uniform for energies in the range of 0.5 to $1.44J/cm_2$. At higher energies, the gold spattered and the imprints become nonuniform as seen in Fig 4.22 below.

As seen in Fig 4.22 the edges of the spot the gold has just spattered around while in the central region uniform deposition is observed. Fig 4.23 shows good quality deposition of the fringe patterns at 20 kHz and the region where the AFM tip was scanned and Fig 4.24 shows its AFM image. As seen in the Figs 4.23 and 4.24 the pitch between line patterns is clearly spaced with distinct peaks. Maximum coverage in terms of thickness ablated from the DS and deposition on AS has been obtained (thickness =50nm). Also the feature line patterns are well defined as seen in optical micrograph denoting good quality deposition.
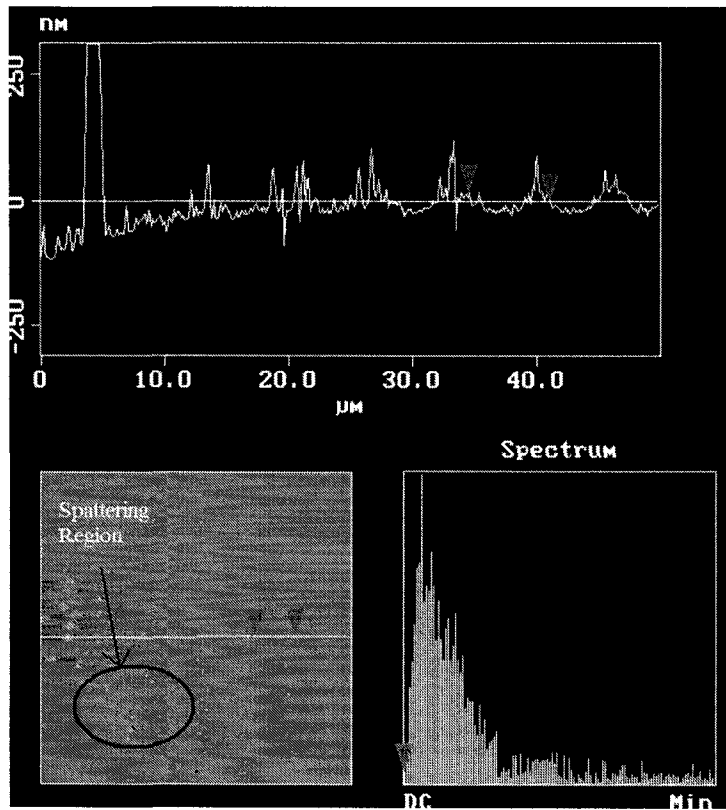
Fig 4.22 Focusing lens of 75.6mm, repetition rate 20 kHz, spoilt gold fringe patterns at

higher energies
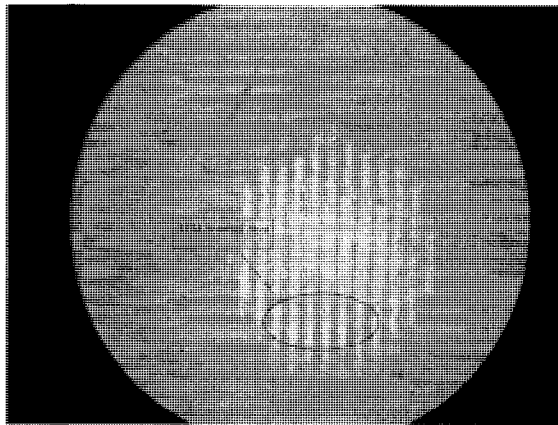
Fig 4.23 Optical Micrograph of fringe pattern deposition at 0.85J/cm², F.O.V=100 μm
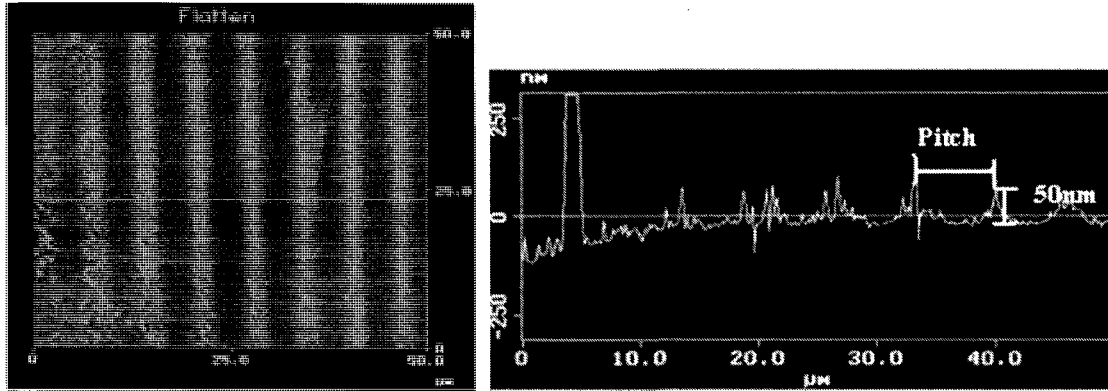
Fig 4.24 AFM image showing fringe pattern deposition at 0.85J/cm2

4.10   Summary

Optimum energy is required for good quality deposition. From the experiments it can be summarized that good quality deposition can be obtained at intermediate fluences. Consequently good coverage in terms of ablated and deposited patterns can be obtained for intermediate fluences. Experiments were also performed by changing the optical setup parameters. Pitch of the fringe patterns i.e. lines ablated and deposited can be easily varied by using different focusing lenses and beam spacing. Pitch of the fringe patterns can be reduced by either increasing beam spacing or decreasing the focal length. Qualities of the line pattern deposition were evaluated by AFM images which confirm good quality deposition at lower and intermediate fluences.

CHAPTER 5   CONCLUSION AND FUTURE WORK

5.1   Conclusion

Microelectronic and biomedical devices require line patterning while its fabrication. LIFT is direct write technique to pattern substrates in ambient condition. Current methods for substrate patterning are expensive and involve many steps. LIFT has not been used for multiple lines patterning which a requirement in many biomedical devices. The proposed method of combining interference principle and Laser Induced Forward Transfer technique will have the ability to pattern lines on a different substrate selectively in a single step.

Predictive modeling has been done to evaluate effect of laser and optical parameters on the dimensions of the line patterns. Refractive index and the thickness of the DS plays an important role in changing dimensions of the patterns ablated and deposited. From the modeling 15 fringes i.e. line patterns are ablated for a fluence of $1.5 J/cm^2$. It can also be predicted that smaller dimensions of line in terms of its width can be obtained by using lenses having lower focal length. As per the modeling, for a DS with thickness of 3mm the pitch between the lines ablated was found to be 7.4 microns. The pitch between the line patterns can be varied by changing the focal length and also by varying beam spacing between the two interfering beams.

A new optical setup has been designed in order to vary the dimension of the line patterns. The setup requires minimum alignment and can be implemented for commercial

applications. Advantage associated with the interference based patterning is that half the laser power is required to ablate and deposit the film on the substrate to be patterned. Experiments were done at different energies in order to study the quality of deposition. Good quality line patterns were obtained for intermediate energies of 1.44J/cm^2 with coverage of up to 80% of the ablated spot size. But at higher energies thinning of line patterns is predominant due to phase transformation of thin film to boiling phase. Experiments were also done to vary the dimension of the line patterns. Minimum of 8 μm pitch obtained was by the lens having focal length of 75.6mm. It was concluded that pitch between the two line patterns can be increased with increase in focusing length or decrease in beam spacing between the two parallel beams and vice versa. Also more energy is required to ablate films with more thickness for good quality deposition. Continuity in the line patterns can be maintained by choosing optimum parameters for scanning the substrate to be patterned. Continuity up to 700 μm was obtained in experiments performed.

5.2   Future Work

Biomedical devices such as stents and catheter require conformal coatings as shown in Fig 1.11. Conformal coatings are patterned across the entire circumference of the device. Liquids and pastes are also used as coating types in this patterning. This work can be further extended for such type of coatings. A rotary stage could be devised where the substrate to be patterned can continually be rotated for film deposition.

In the experiments performed the deposition quality depends on the number of laser pulses hitting the target and also its pulse width. All the experiments were performed keeping time=1sec for ablation and deposition. In order to control the dimension of the line patterns, its ablation and deposition should be controlled. This can be done by controlling the number of pulses hitting the substrate. Electronic shutters can be used to control the number of pulses hitting the DS, especially at higher repetition rates.

LIFT involves complex dynamics while the film is ablating and getting deposited on the AS. The exact dynamics for mechanism of ablation in LIFT still is a topic of research. Further simulation work can be done to study this mechanism of film ablation with interference principle.

References

[1]http://www.memsnet.org/mems/processes/lithography.html

[2]B. Bushan; "Ed. Springer Handbook of Nanotechnology Berlin", Germany: Springer–Verlag, 2004.

[3]http://www.fractal.org/Fractal-Research-and-Products/Nano-patterning.htm

[4]http://www.wwnorton.com/college/chemistry/chemconnections/Chip/pages/photo_.html

[5]R.S. Kane, S. Takayama, E. Ostuni, D.E. Ingber and G.M. Whitesides, "Patterning proteins and cells using soft lithography", Biomaterials 20 pp. 2363–2376, 1999.

[6]S. K. Ghandhi, "VLSI Fabrication Principles: Silicon and Gallium Arsenide", 2nd ed. New York: Wiley, 1994.

[7]Y. Xia, J. A. Rogers, K. E. Paul and G. M. Whitesides, "Unconventional methods for fabricating and patterning nanostructures",Chem. Rev. 99 pp.1823-1848,1999.

[8]M. DiVentra, S. Evoy and J. R. Heflin, "Introduction to nanoscale science and technology", Kluwer Academic Publishers, 2004.

[9]Xia, Y. and Whitesides, G. M. Annu, "Soft Lithography", Rev. Mater. Sci.28, 153-184, 1998.

[10]http://www.research.philips.com/technologies/light_dev_microsys/softlitho/index.html

[11]A. Kumar, G. M. Whitesides, Applied Physics Letters, Vol. 63, 2002-2004,1993.

[12]A. Piqué, D.B.Chrisey (Eds.) "Direct-write Technologies for Rapid Prototyping Applications", Academic Press, San Diego, 2002.

[13]S. Jeon, E. Menard, J-U. Park, J. Maria, M. Meitl, J. Zaumseil and J. A. Rogers, "Threedimensional nanofabrication with rubber stamps and conformable photomasks", Adv.Mater., 16 pp.1369-1373, 2004.

[14]W. R. Childs and R .G. Nuzzo, "Decal transfer microlithography: a new softlithographic patterning method", J. Am. Chem. Soc. 124 45, pp.13583-13596, 2002.

[15]Y-L. Loo, R. L. Willett, K. W. Baldwin and J. A. Rogers, "Interfacial chemistries for nanoscale transfer printing", J. Am. Chem. Soc. 124,26, pp.7654 –7655, 2002.

[16]D.J. Ehrlich and J.Y.Tsao, "Laser Microfabrication", (Academic Press, Inc., New York, NY, 1989.

[17]http://www.emeraldinsight.com/Insight/ViewContentServlet?Filename=Published/E meraldFullTextArticle/Articles/0330250406.html

[18]Auyeung Raymond et al.,"Laser forward transfer of rheological systems" US Patent 6805918, 2004.

[19]Bohandy, J., Kim B.F., and Adrian, F.J., "Metal deposition from a supported metal film using an excimer laser," Journal of Applied Physics, Vol. 60, No. 4, pp. 1538-1539, 1986.

[20]M. Duocastella, M. Colina, J.M. Fernández-Pradas, P. Serra, J.L. Morenza, "Study of the laser-induced forward transfer of liquids for laser bioprinting", Applied Surface Science, 253, 7855 7859, 2007.

[21]Vicentiu Grosu "Lift Heat Transfer Analysis of Nanosecond Laser-Induced Forward Transfer", PhD Thesis, 2005.

[22]Mogyorósi, P., Szörényi, T., Bali, K., Tóth, Zs. & Hevesi, I," Pulsed laser ablative deposition of thin metal films"Appl. Surf. Sci. 36, 157–166, 1989.

[23]V.P. Veiko, E.A. Shakhno, V.N. Smirnov, A.M. Miaskovski, And G.D. Nikishin,"Laser–induced film deposition by LIFT: Physical mechanisms and applications" Laser and Particle Beam, 24, 203–20, 2006.

[24]Bohandy, J., Kim B.F., Adrian, F.J., and Jette A. N., "Metal deposition at 532 nm using a laser transfer technique," Journal of Applied Physics, Vol. 63, No. 4, pp. 1158-1162, 1987.

[25]Baseman, R.J., Gupta, A., Sausa R.C., and Progler, C., and Watson, T.J., "Laser induced forward transfer," Materials Research Society Symposium Proceedings, Vol. 101, pp. 237-242, 1988.

[26]Fogarassy, E., and Fuchs, C., "Laser-induced forward transfer: A new approach for the deposition of high-TC supercoating thin films" Journal of Materials Research, Vol. 4, No. 5, pp. 1082-1086, 1989.

[27]Fogarassy, E., and Fuchs, C., "Laser-induced forward transfer: A new approach for the deposition of high-TC supercoating thin films" Journal of Materials Research, Vol. 4, No. 5, pp. 1082-1086, 1989.

[28]Kantor, Z., Toth, Z., and Szorenyi, T., "Laser Induced Forward Transfer: The effect of support-film interface and film-to-substrate distance on transfer," Applied Physics A, Vol. 54, pp. 170-175, 1992.

[29]Bullock, A.B., and Bolton P.R., "Laser-induced back ablation of aluminum thin film using ultrashort laser pulses," Conference on Lasers and Electro-Optics Pacific Rim '97, pp. 98-99, 1997.

[30]Bullock, A.B., and Bolton P.R., "Laser-induced back ablation of aluminum thin film using picosecond laser pulses," Journal of Applied Physics, Vol. 85, No. 1, pp. 460-465, 1999.

[31]Zergioti, I., Mailis, S., Vainos, N.V., Papakonstantinou, P., Kalpouzos, C., Grigoropoulos, C. P., and Fotakis, C., "Microdeposition of metal and oxide structures using ultrashort laser pulses," Applied Physics A, Vol. 66, pp. 579-582, 1998.

[32]Yamada, H., Sano, T., Nakayama, T. & Miyamoto, I" Optimization of laser-induced forward transfer process of metal thin films" Applied Surface Science 197-198, 411-415, 2002.

[33]Sano, T., Yamada, H., Nakayama, T. & Miyamoto, I,"Experimental investigation of laser induced forward transfer process of metal thin films" Applied Surface Science 186, 221-226, 2002.

[34]P. Serra, J.M. Fernández-Pradas, F.X. Berthet, M. Colina, J. Elvira and J.L. Morenza "Laser direct writing of biomolecule microarrays", Appl. Phys. A 79, pp. 949–952, 2004.

[35]J.M. Fernández-Pradas, M. Colina, P. Serra, J. Domínguez and J.L. Morenza, "Laser-induced forward transfer of biomolecules", Thin Solid Films 453–454, pp. 27–30, 2004.

[36]M. Colina, P. Serra, J.M. Fernández-Pradas, L. Sevilla and J.L. Morenza," DNA deposition through laser induced forward transfer", Biosens. Bioelectron. 20 , p. 1638, 2005.

[37]M. Colina, M. Duocastella, J. M. Fernández-Pradas, P. Serra,a_ and J. L. Morenza ,"Laser-induced forward transfer of liquids: Study of the droplet ejection process", Journal of applied physics, v. 99,no.p.084909, 2006.

[38]Sudipta Bera, A. J. Sabbah, J. M. Yarbrough, C. G. Allen, Beau Winters, Charles G. Durfee, and Jeff A. Squier," Optimization study of the femtosecond laser-induced forward-transfer process with thin aluminum films", Applied Optics Vol. 46, No. 21; 2007.

[38]Ready J. "Lasers- Their Unusual Properties and Their Influence on Application", Lasers in Modern Industry, Society of Manufacturing Engineers Marketing Services Dept., Dearborn, MI, 17-38, 1979.

[39]http://kottan-labs.bgsu.edu/teaching/workshop2001/chapter4a.htm

[40]http://www.semrock.com/TechNotes/TN_LaserDamageThreshold.htm

[41]Meijer, J., Du, K., Gillner, A., Hoffmann, D., Kovalenko, V.S., Masuzawa, T., Ostendorf, A.,Poprawe, R., and Schulz, W., "Laser machining by short and ultrashort pulses, state of the art and new opportunities in the age of the photons," Annals of the CIRP, 51/2, 531-652, 2002.

[42]Grigoropoulos, C.P., Bennett, T.D., Ho, J.R., Xu, X.,and Zhang, X., "Heat and mass transfer in pulsed-laser-induced phase transformation," Advances in Heat Transfer, 28, 75-134, 1996

[43]Ivanov, D., and Zhigilei, S., "Combined atomistic-continuum modeling of short-pulse laser melting and disintegration of metal films," Physical Review B, 68, 1-22, 2003.

[44]http://www.semrock.com/TechNotes/TN_LaserDamageThreshold.htm

[45]http://www.mellesgriot.com/products/optics/gb_2_1.htm

[46]http://www.rp-photonics.com/beam_quality.html

[47]Kenneth Barat, Laser Safety Management (CRC Press), 267 pages, 2006.

[48]Sinzinger S and Jahns J, "Microoptics", (New York: Wiley), 1999.

[49]C. Scha" fer and H. M. Urbassek, "Metal Ablation by Picosecond Laser Pulses: A Hybrid Simulation", Phys. Rev. B, vol. 66, 115404, 2002.

[50]http://www.inst.bnl.gov/programs/laseropt/lasers/micromach.shtml

[51]T.Q. Jia, H.X. Chen, M. Huang, F.L. Zhao, J.R. Qiu, R.X. Li, Z.Z. Xu,X.K. He, J. Zhang, H. Kuroda, "Formation of nanogratings on the surface of a ZnSe crystal irradiated by femtosecond laser pulses", Phys. Rev. B 72 125429, 2005.

[52]N. H. Rizvi, "Femtosecond laser micromachining: Current status and applications," Riken Rev. 50, 107-112, 2003.

[53]http://www.tamsci.com/products/ablation2.html

[54]Suraj Kabadi,' "Advanced Fabrication of Electroactive Nanowell Sensors", Biological Applications , Research Accomplishments, NNIN REU, 2006.

[55]KM Merdan, VN Shapovalov, "Laser deposition of elements onto medical devices", US 6,723,390, 2002.

[56]W.L. Liang et al., "Micromachining of circular ring microstructure by femtosecond laser pulses" Optics & Laser Technology 35 (2003) 285 – 290.

[57]http://jolisfukyu.tokai-sc.jaea.go.jp/fukyu/tayu/ACT04E/05/0501.htm

[58]D. Bäuerle, J. D. Pedarnig, I. Vrejoiu, M. Peruzzi, D. G. Matei, D. Brodoceanu, " Laser Processing And Chemistry: Applications In Nanopatterning", Material Synthesis And Biotechnology, Romanian Reports In Physics, Vol. 57, No. 4, P. 935–952, 2005.

[59]Kawamura K, Sarukura N, Hirano M, Ito N, Hosono H., "Periodic nanostructure array in crossed holographic gratings on silica glass by two interfered infrared-femtosecond laser pulses", Appl Phys Letter, 79(9):1228–30, 2001.

99

[60]Kawamura K, Sarukura N, Hirano M, Hosono H., "Holographic encoding of permanent gratings embedded in diamond by two beam interference of a single femtosecond near-infrared laser pulse" Japanese J Appl Phys, 39:L767–9, 2000.

[61]Zhai J, Shen Y, Si J, Qiu J, Hirao K., "The fabrication of permanent holographic gratings in bulk polymer medium by a femtosecond laser", J Phys D,34:3466-9, 2001

[62]Oi K, Barnier F, Obara M., "Fabrication of Gber Bragg grating by femtosecond laser interferometry", Proceedings of the Conference of LEOS, San Diego, California, vol. 2, p. 776–7, 2001.

[63]Zhao, J. Qiu, C. Zhao, W. Jiang and C. Zhu, "Optical transfer of periodic microstructures by interfering femtosecond laser beams", Opt. Express 13, p. 3104, 2005.

[64]Toshiaki Kondo, Shigeki Matsuo,a) Saulius Juodkazis, Vygantas Mizeikis,b) and Hiroaki Misawa, "Multiphoton fabrication of periodic structures by multibeam interference of femtosecond pulses" Appl. Phys. Lett., Vol. 82, No. 17, 28, 2003.

[65]L. Landström, J. Klimstein, G. Schrems, K. Piglmayer, D. Bäuerle, "Single-step patterning and the fabrication of contact masks by laser-induced forward transfer", Appl. Phys., A 78, 537, 2004.

[66]B.N. Chicbkov, C. Momma, S. Nolte, F. yon Alvensleben, A. Tiinnermann, "Femtosecond, picosecond and nanosecond laser ablation of solids", Appl. Phys. A 63, 109, 1996.

[67]http://en.wikipedia.org/wiki/Gaussian_beam

[68]Yas A. Alsultanny, " Laser Beam Analysis Using Image Processing", J. Computer Sci., 2 (1): 109-113, 2006.

[69]John F. Ready (Editor in Chief), Dave F. Farson (Associate Editor), "LIA handbook of laser materials processing", Laser Institute of America/Magnolia Publishing/Springer, Berlin, 2001.

[70]Gasvik, K. J., "Optical Metrology", Wiley, Chichester, 1987.

[71]Kęstutis Regelskis, Gediminas Račiukaitis and Mindaugas Gedvilas, "Ripple formation in the chromium thin film during laser ablation" appl. Surf. Sci. ,v. 253 ,6584, 2007.

[72]K.Venkatakrishnan et. al, "Direct fabrication of surface-relief grating by interferometric technique using femtosecond laser", Appl. Phys. A 77, 959–963, 2003.

[73]H., Yamada, T., Sano, T., Nakayama, and I. Miyamoto, "Optimization of laser-induced forward transfer process of metal thin films", Appl. Surf. Sci. 197-198, 411-415, 2002.

[74]Bo Tan, Narayanswamy R Sivakumar and Krishnan Venkatakrishnan, " Direct grating writing using femtosecond laser interference fringes formed at the focal point", J. Opt. A: Pure Appl. Opt.7, 169–1747, 2005.

[75]http://www.umms.sav.sk/index.php?ID=415

[76] Varel, H., Ashkenasi, D., Rosenfeld, A., Herrmann, R., Noack, F., and Campbell, E. E. B., "Laser-induced damage in SiO2 and CaF2 with picosecond and femtosecond laser pulses", Applied Physics a-Materials Science & Processing, 62, 293-294, 1996.

[77]Hoshino, K., "Electrowetting-based pico-liter liquid actuation in a glass-tube microinjector", Sensors and Actuators A:Physical   v. 114   no. 2-3   p. 473, 2004.

[78]http://www.coherent.com/Lasers/index.cfm?fuseaction=show.page&ID=1433

[79]http://www.altechna.com/product_details.php?id=361

[80]http://www.newport.com/servicesupport/Tutorials/default.aspx?id=118

[81]Emily Kubacki, "Waveplates offer precise control of polarization", Product Guide, www.optics.org/ole, 2006.

[82]http://www.deoslaser.com/Lasers/index.cfm?fuseaction=show.page&id=1591&loc=8 30

[83]http://www.newport.com/store/genproduct.aspx?id=139709&lang=1033&Section=D etail

[84]http://search.newport.com/?sku=G3978

[85]Miotello, A. and Kelly, R., "Critical assessment of thermal models for laser Sputtering at high fluences," *Applied Physics Letter*, Vol. 67, pp. 3535-3537, 1995.

Appendix 1

Average Laser Pulse Power

Power of the laser at different rep rates (KHz) and diode currents (A):

	20kHz	30kHz	40kHz	50kHz	60kHz	70kHz	80kHz	90kHz	100kHz
18A	1.7	1.8	1.9	1.9	1.9	1.9	2.0	2.0	2.0
19A	2.66	2.77	2.92	3.00	3.18	3.19	3.20	3.25	3.28
20A	3.0	3.2	3.3	3.35	3.4	3.45	3.5	3.5	3.5
21A	4.22	4.5	4.68	4.8	5.00	5.1	5.12	5.3	5.41
22A	4.7	4.8	5.1	5.15	5.3	5.33	5.4	5.44	5.5
23A	6.02	6.6	6.81	7.0	7.41	7.44	7.55	7.6	7.8
24A	6.6	6.9	7.5	7.6	7.7	7.7	7.9	7.9	7.9
25A	7.7	8.1	9.30	9.65	9.75	10.00	10.1	10.6	10.70
26A	8.3	9.0	10.2	10.25	10.5	10.55	10.7	10.8	10.8
27A	9.12	9.5	11.70	12.1	12.50	12.59	12.99	13.21	13.30
28A	9.6	10.00	12.5	12.5	13.0	13.1	13.2	13.3	13.4
29A	10.34	12.00	13.50	13.70	14.60	14.8	15.12	15.13	15.23
30A	10.4	12.1	14.2	14.3	14.9	14.9	15.00	15.15	15.3
31A	10.6	12.9	15.00	15.45	16.00	16.05	16.2	16.30	16.4
32A	10.8	13.1	15.2	15.5	16.1	16.1	16.3	16.5	16.6